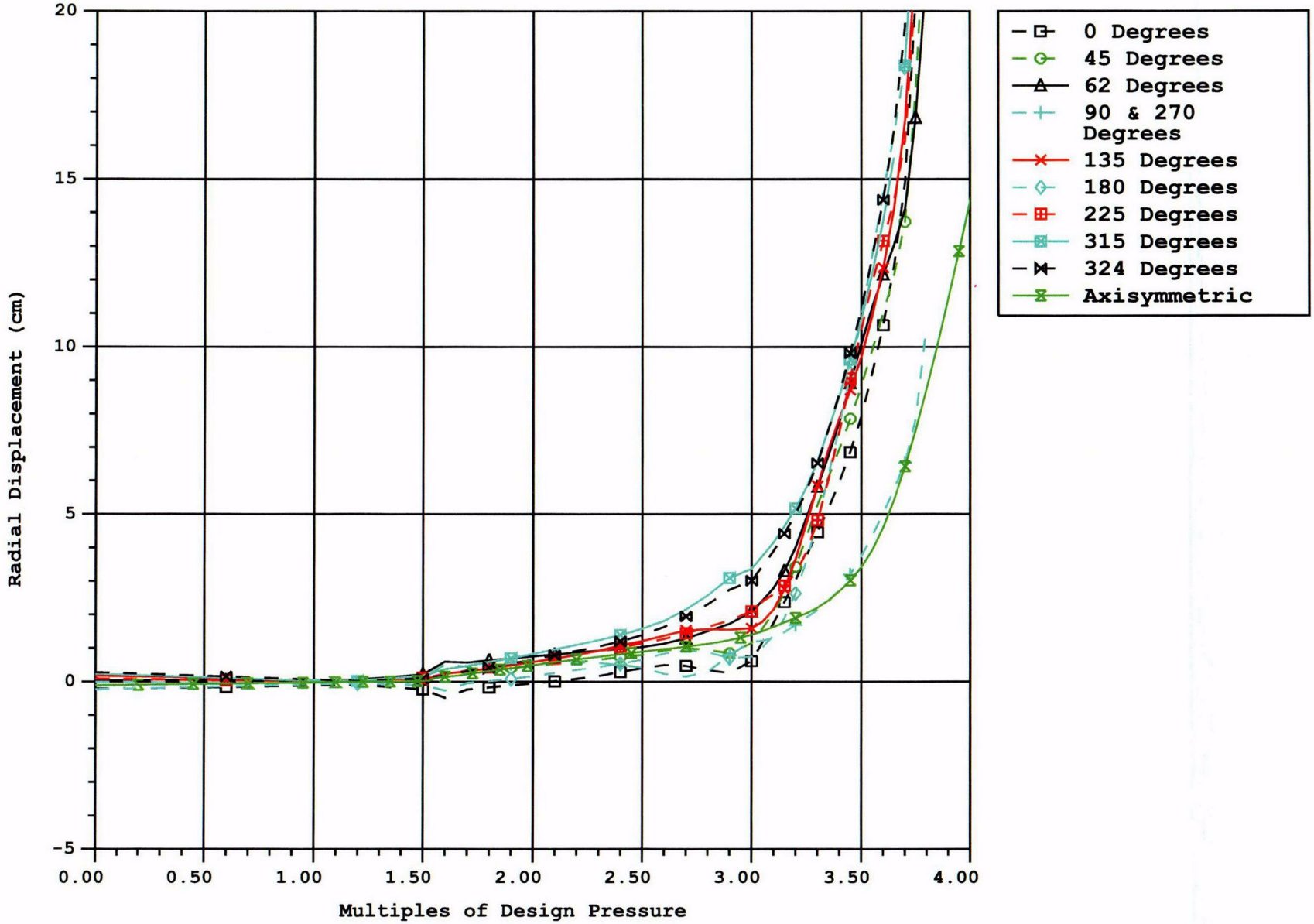

Figure 6-13. Radial Displacement at Elevation 8.9M, 3DCM Run 5 Compared to Axisymmetric

C115

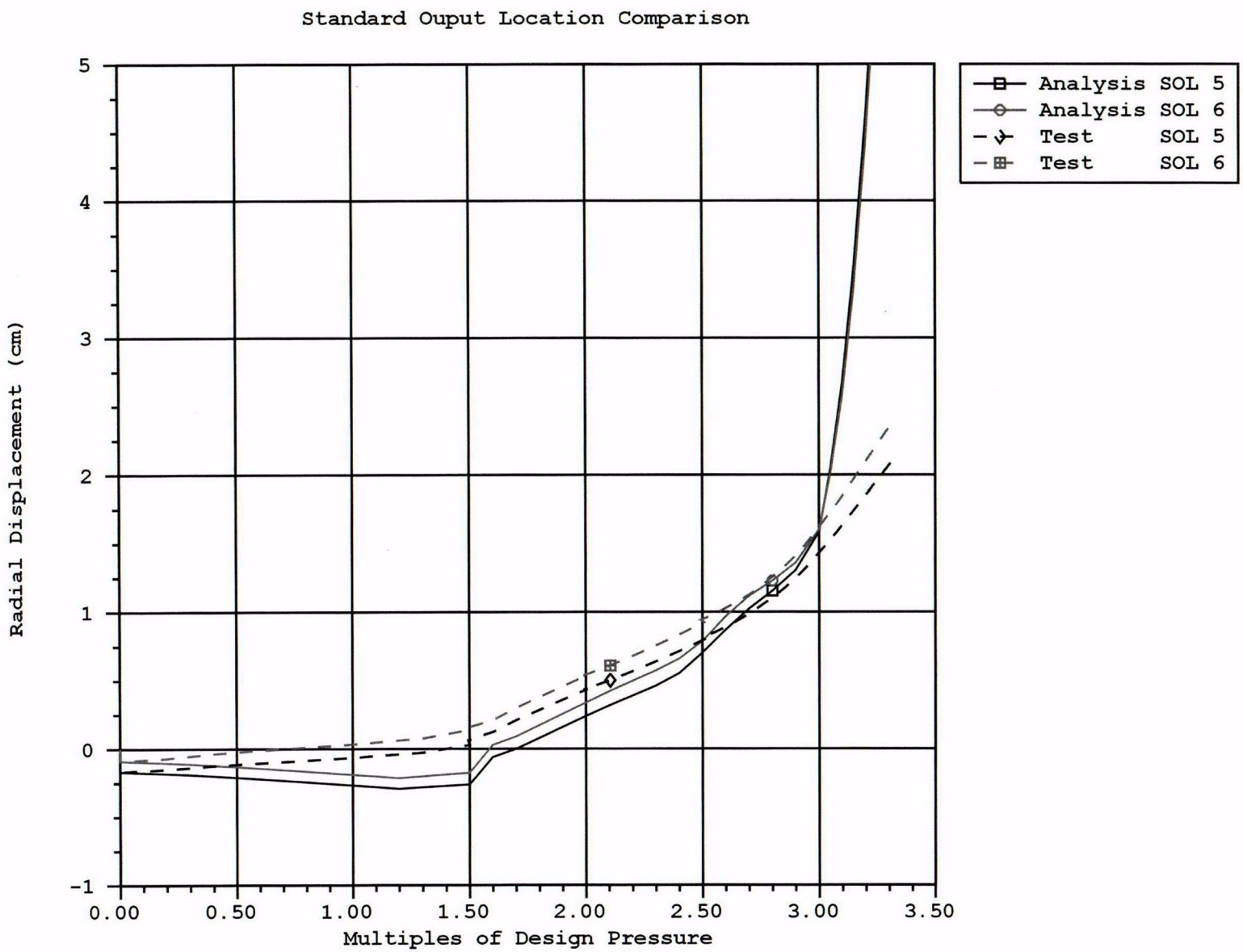

Figure 6-14. Comparison of Run 4 SOL 5 and 6 (Radial Displacement at 135 Degrees, 4.7M, 6.2M)

C116

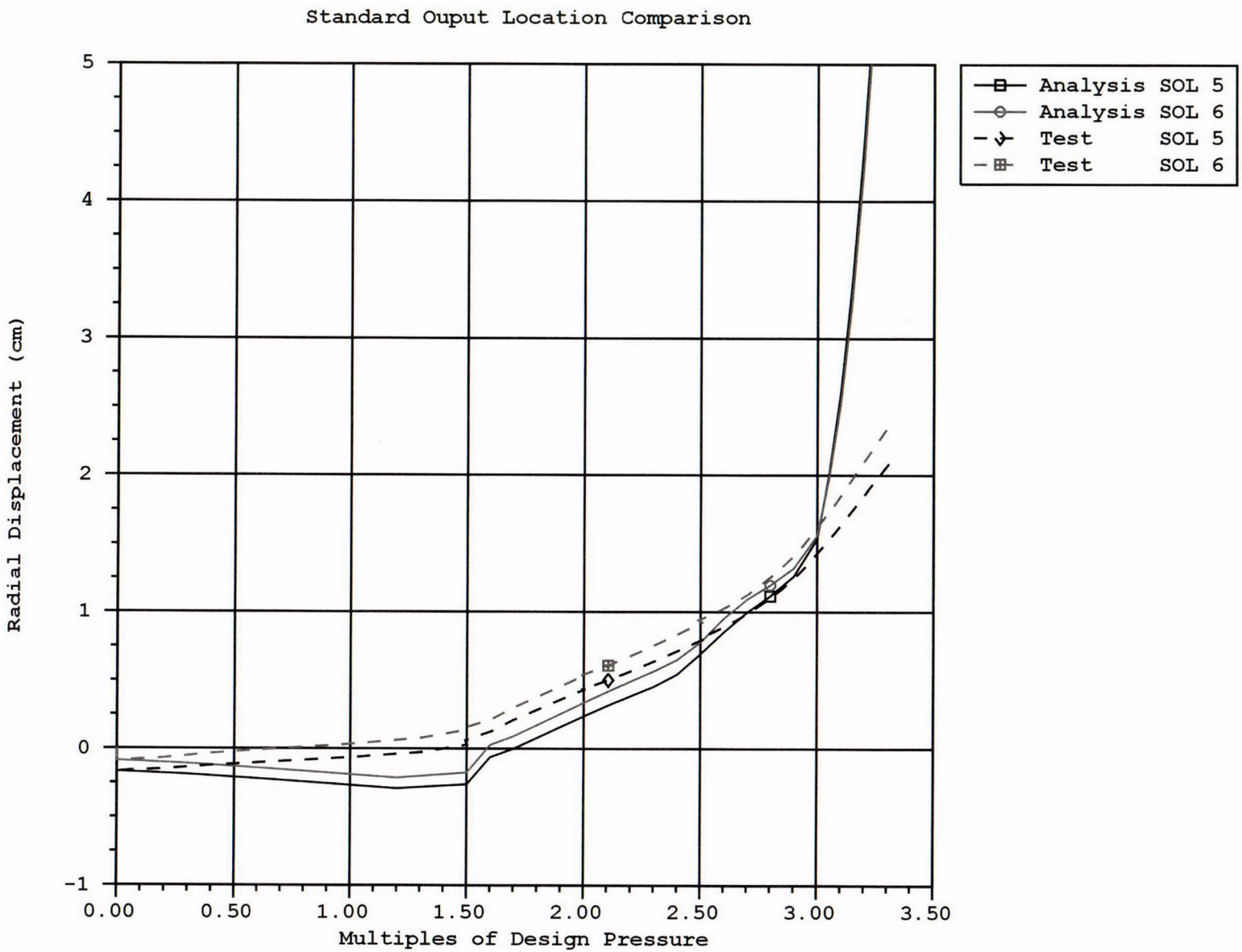

Figure 6-15. Comparison of Run 5 SOL 5 and 6 (Radial Displacement at 135 Degrees, 4.7M, 6.2M)

C117

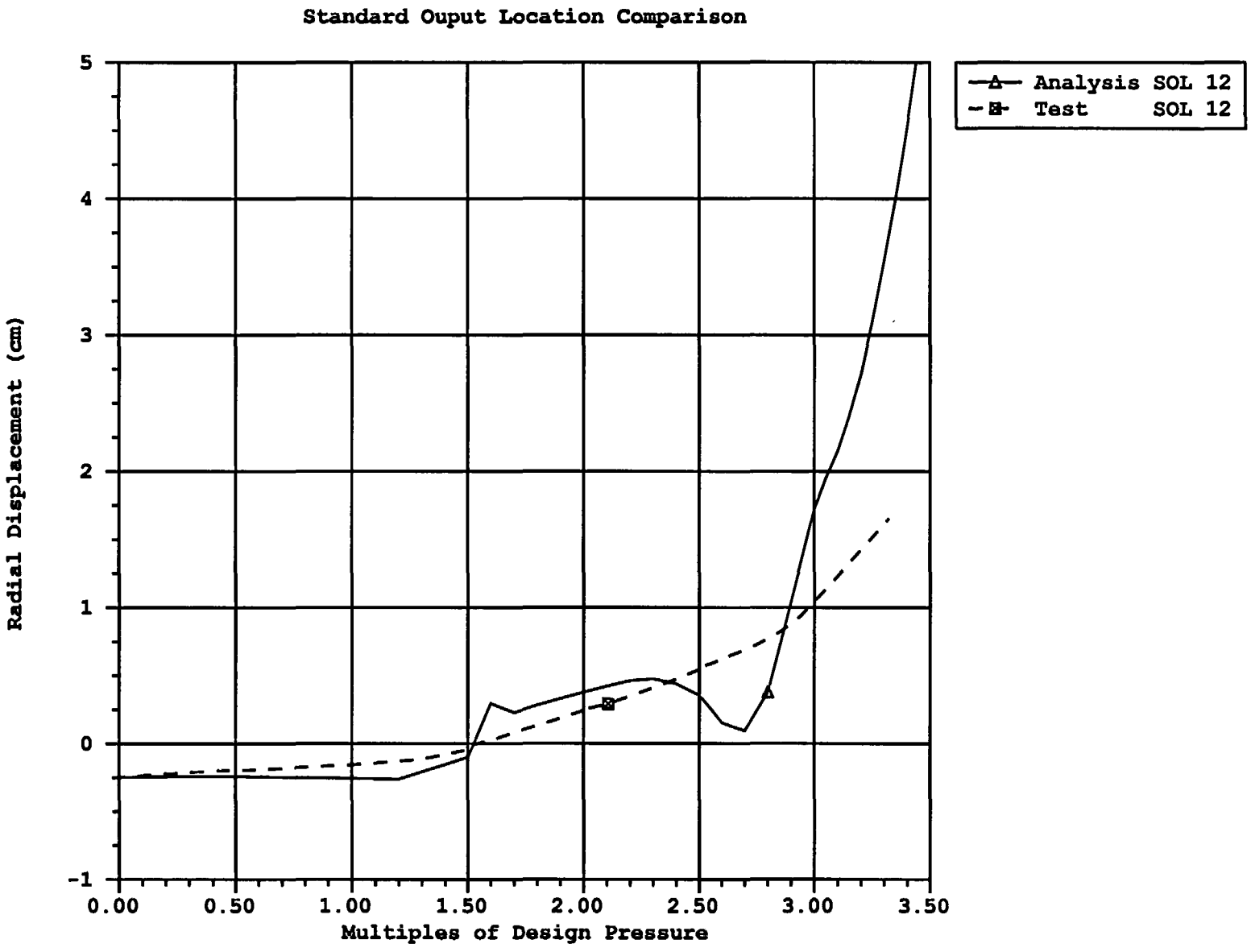

Figure 6-16. Comparison of Run 4 SOL 12 (Radial Displacement at 90 Degrees Butress, 6.2M)

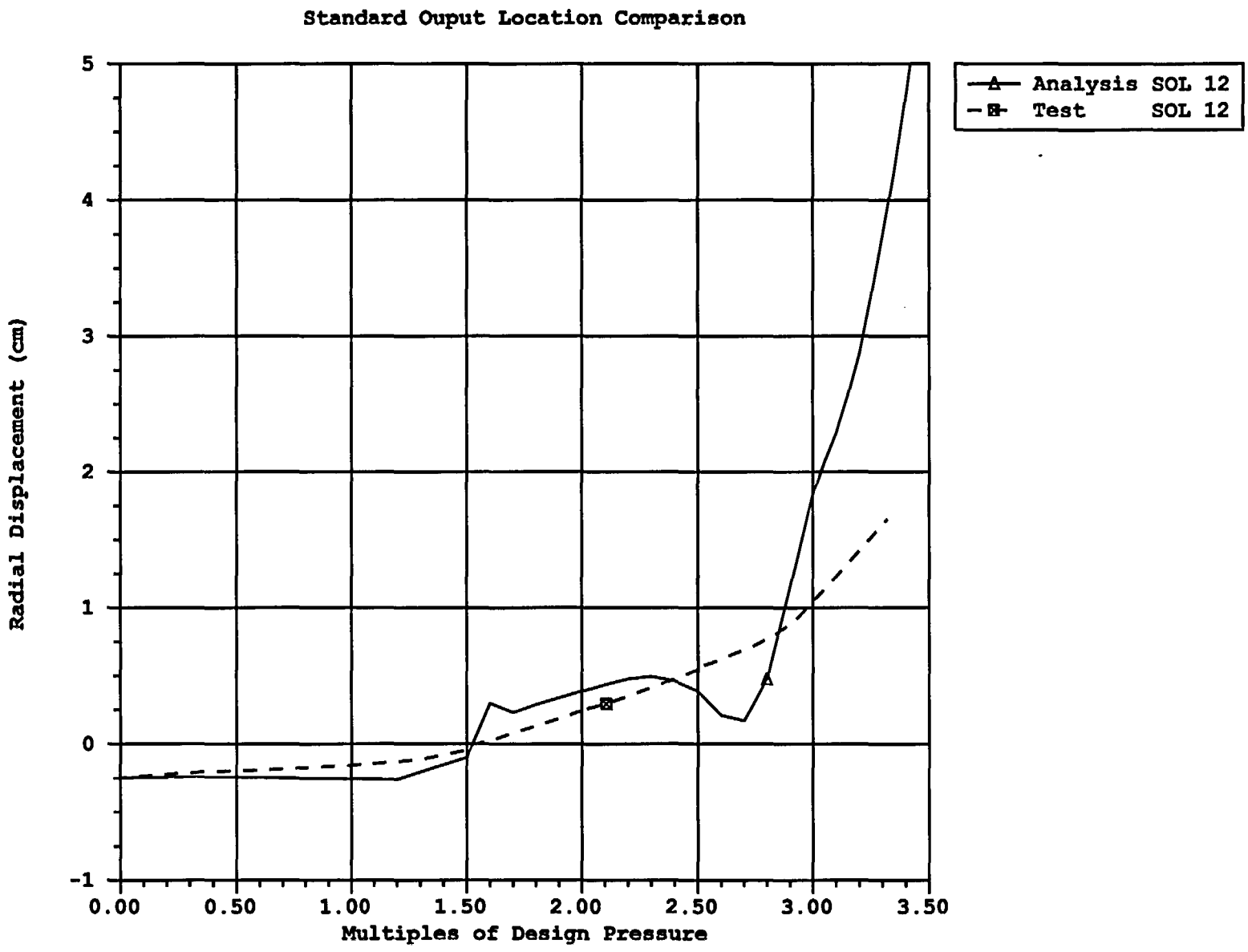

Figure 6-17. Comparison of Run 5 SOL 12 (Radial Displacement at 90 Degrees Butress, 6.2M)

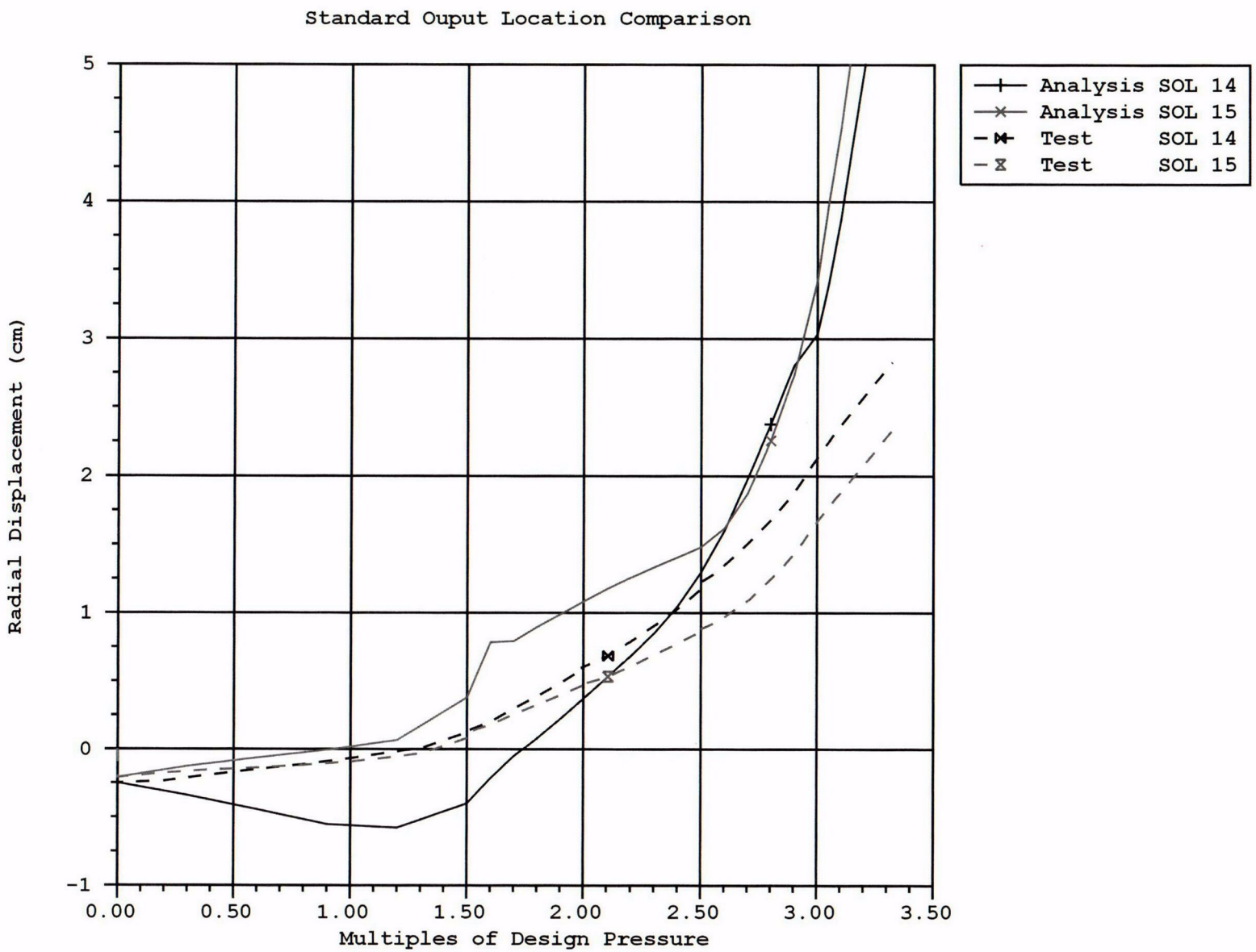

Figure 6-18. Comparison of Run 4 SOL 14 and 15 (Radial Displacement at E/H and A/L)

C118

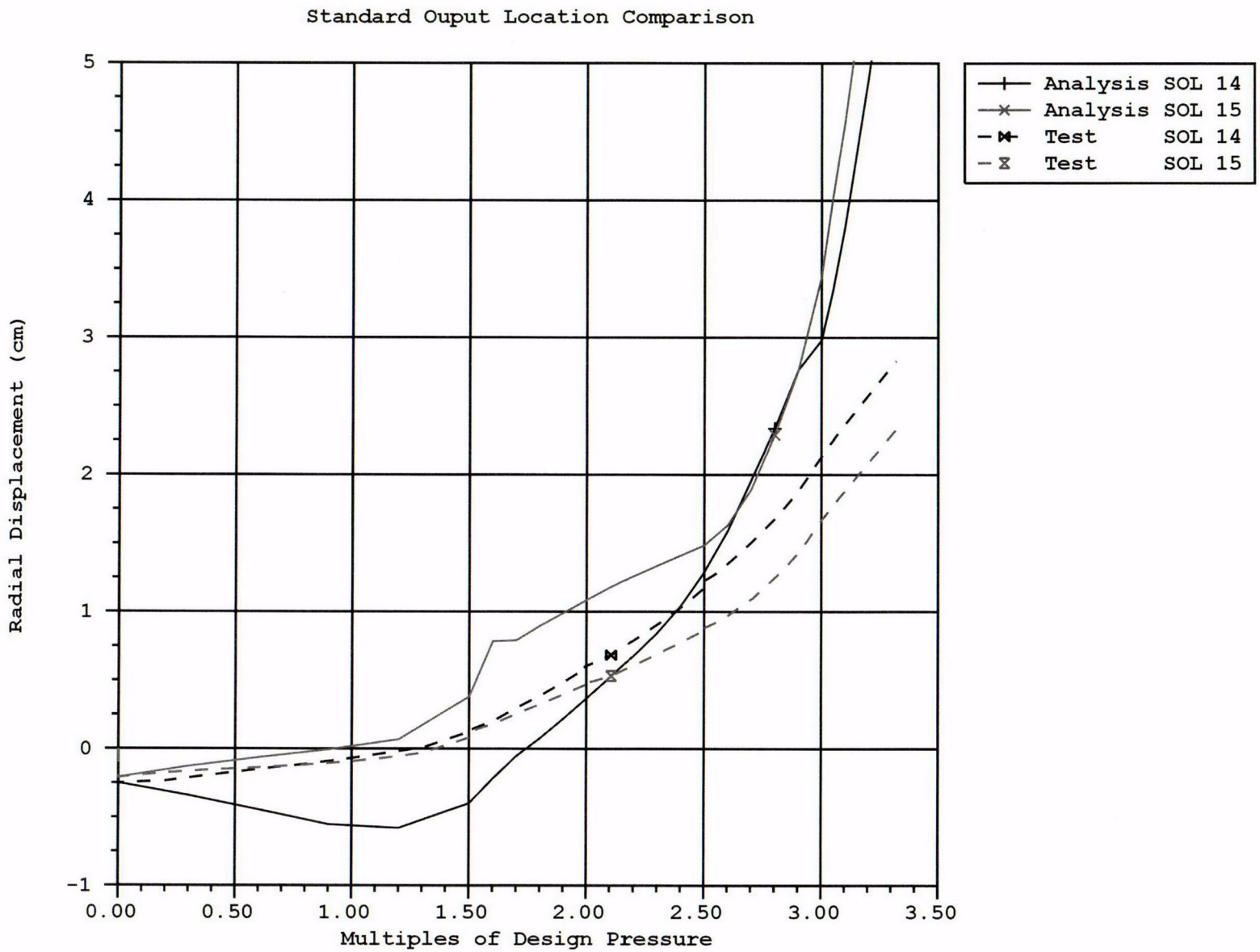

Figure 6-19. Comparison of Run 5 SOL 14 and 15 (Radial Displacement at E/H and A/L)

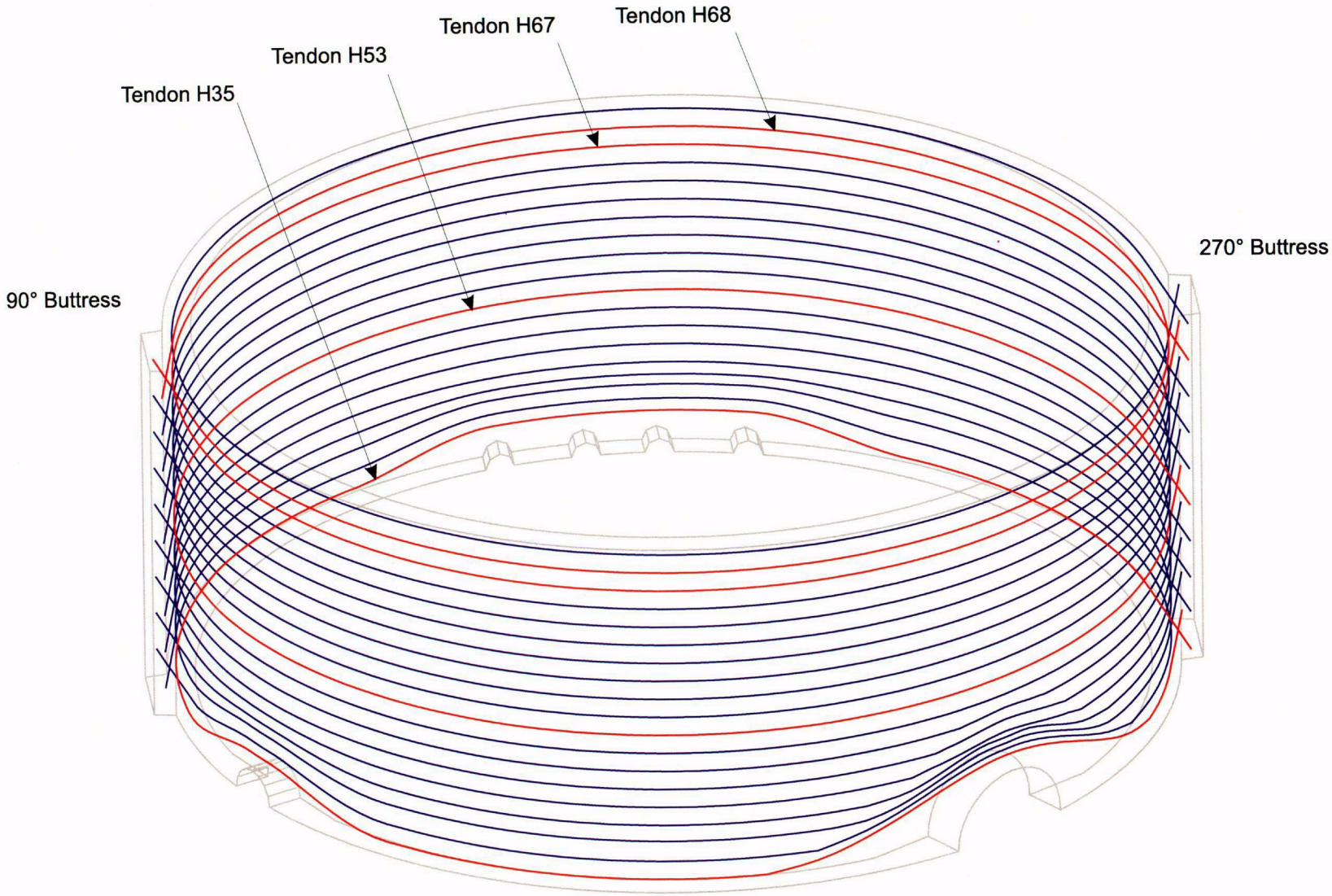

Figure 6-20. Location of Instrumented Tendons H35, H53, H67, and H68

C120

Step 1. Apply Post-Tensioning with Original Friction Element Modeling

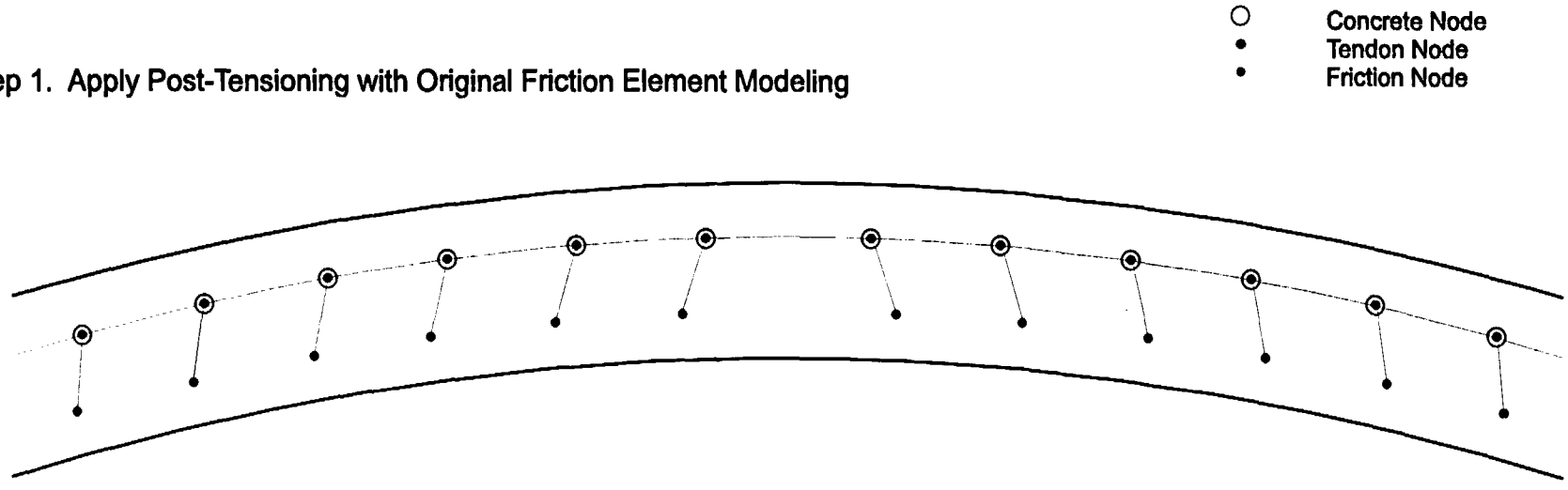

Step 2. After Post-Tensioning Lock-in Post-Tension effects.
- Remove Friction Elements
- Numerically Constrain Tendon Nodes to Concrete Nodes in Deformed Position

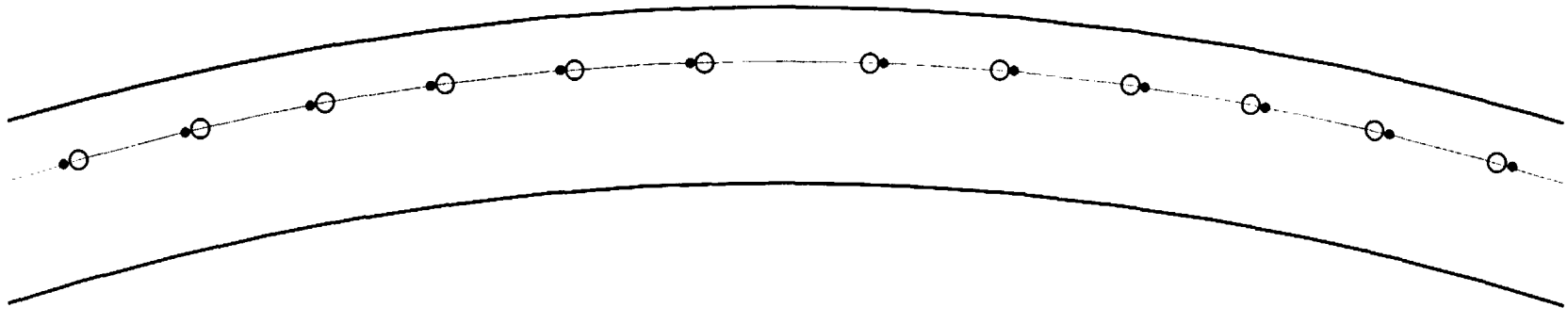

Figure 6-21. Tendon Friction Modeling Schematic for Run 6

Step 1. Apply Post-Tensioning with Original Friction Element Modeling

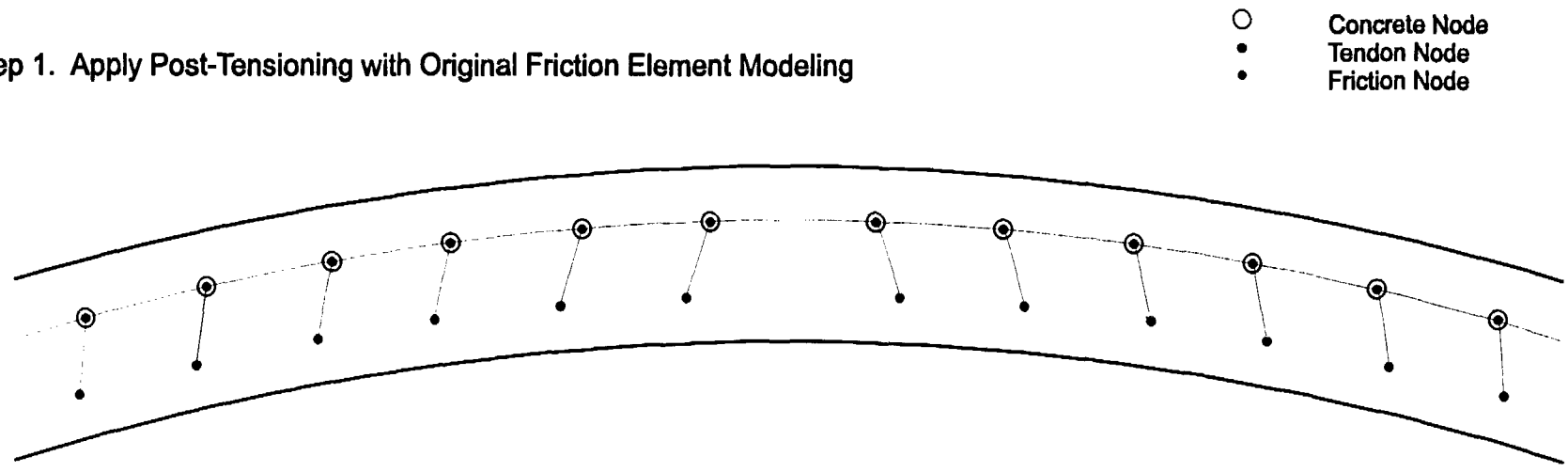

Step 2. At 1.5 Pd Realign Friction Elements to Radial Position - No Friction Assumption

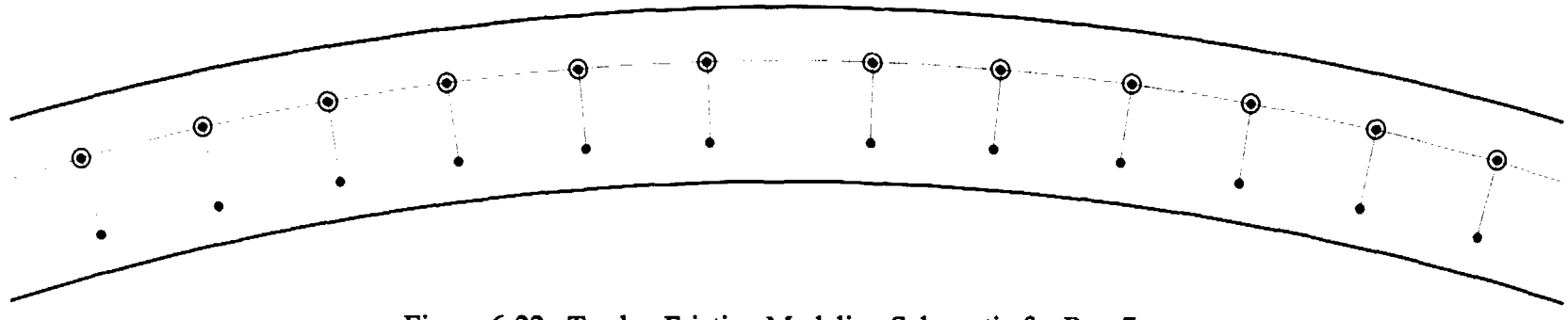

Figure 6-22. Tendon Friction Modeling Schematic for Run 7

Step 1. Apply Post-Tensioning with Original Friction Element Modeling

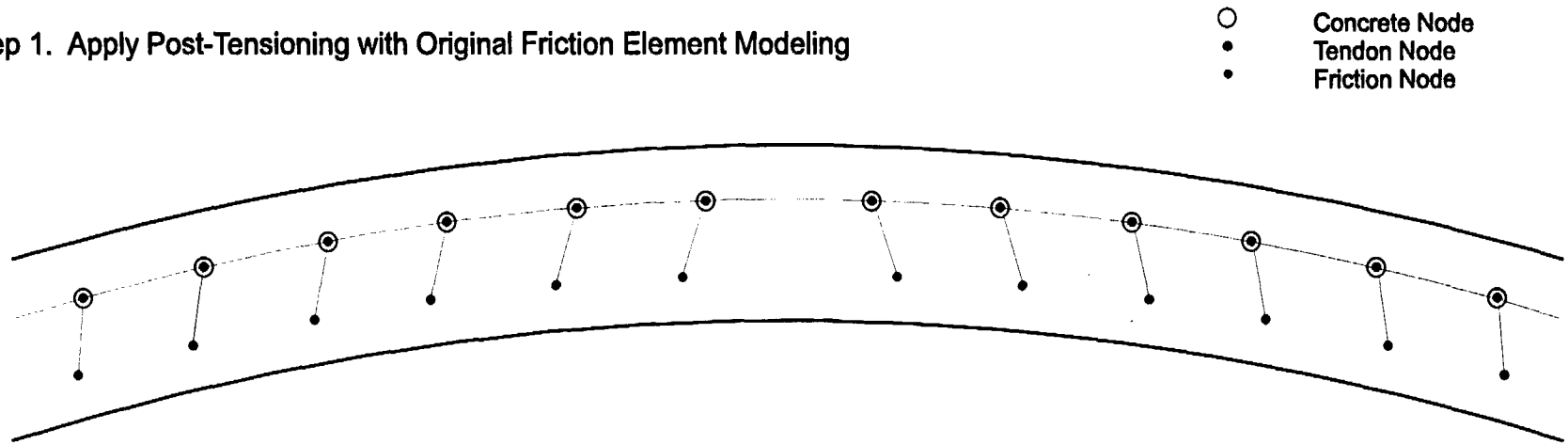

Step 2. After Post-Tensioning Add Second Series of Friction Elements Strain Free with Opposite Orientation

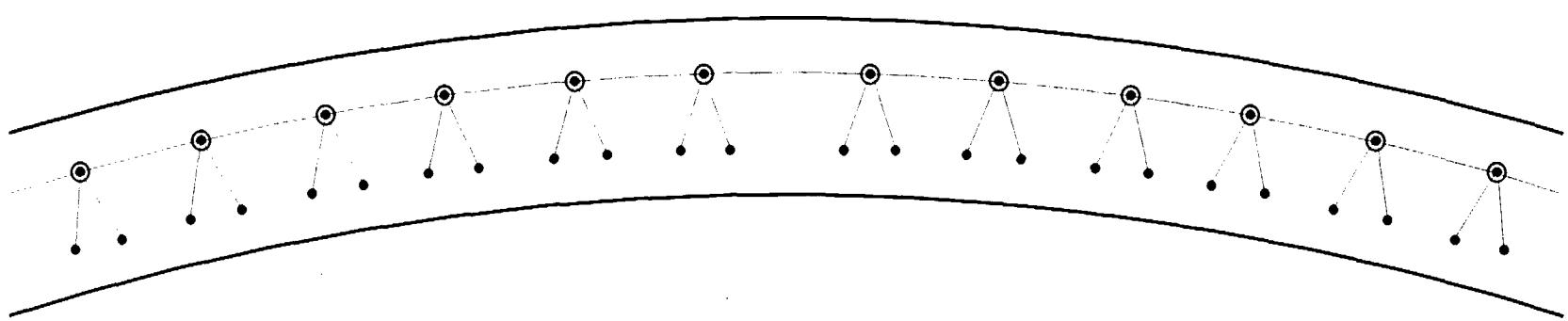

Figure 6-23. Tendon Friction Modeling Schematic for Run 9

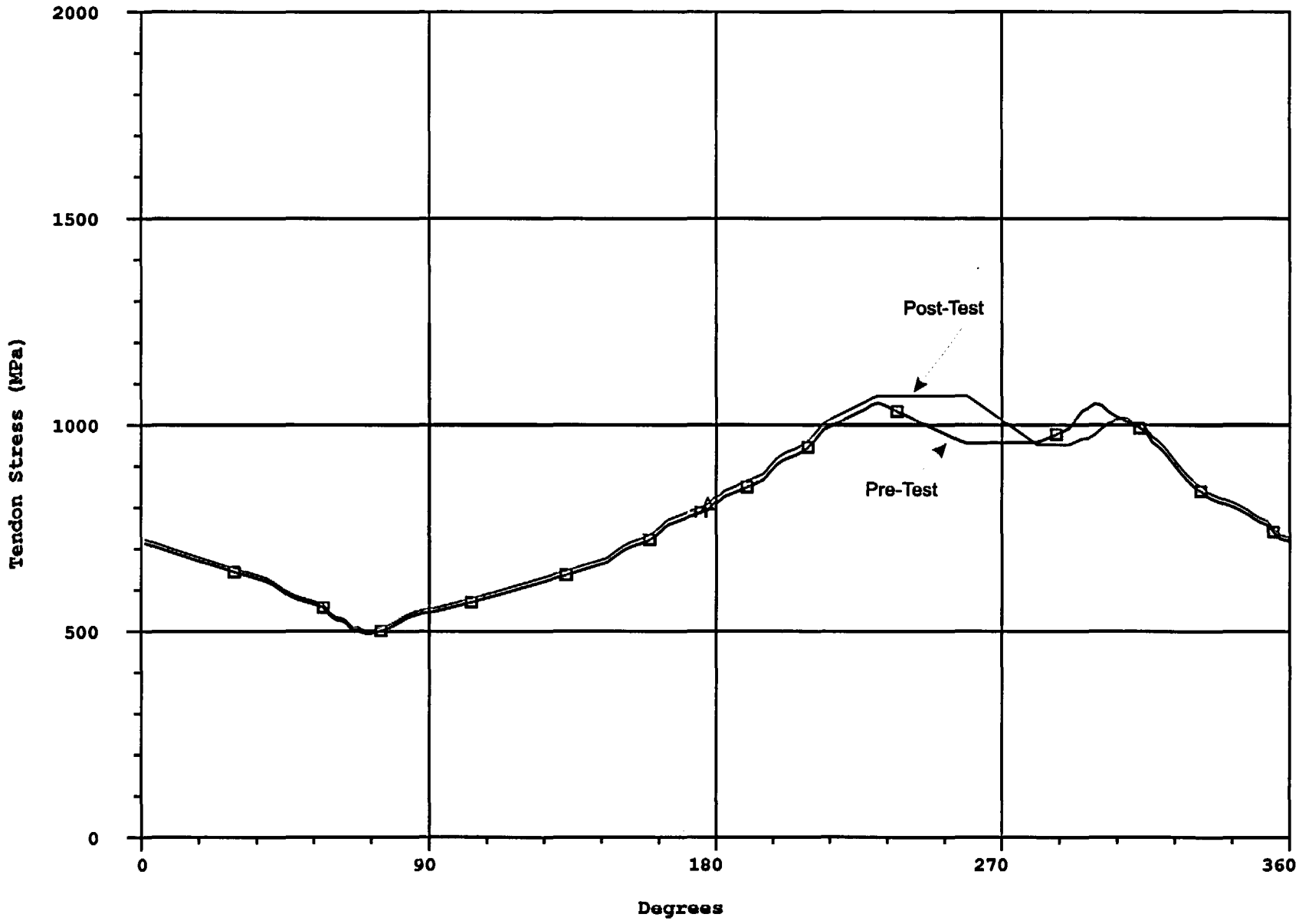

Figure 6-24. Changes to Anchor Set Prestress for Posttest 3DCM Study, Tendon H35

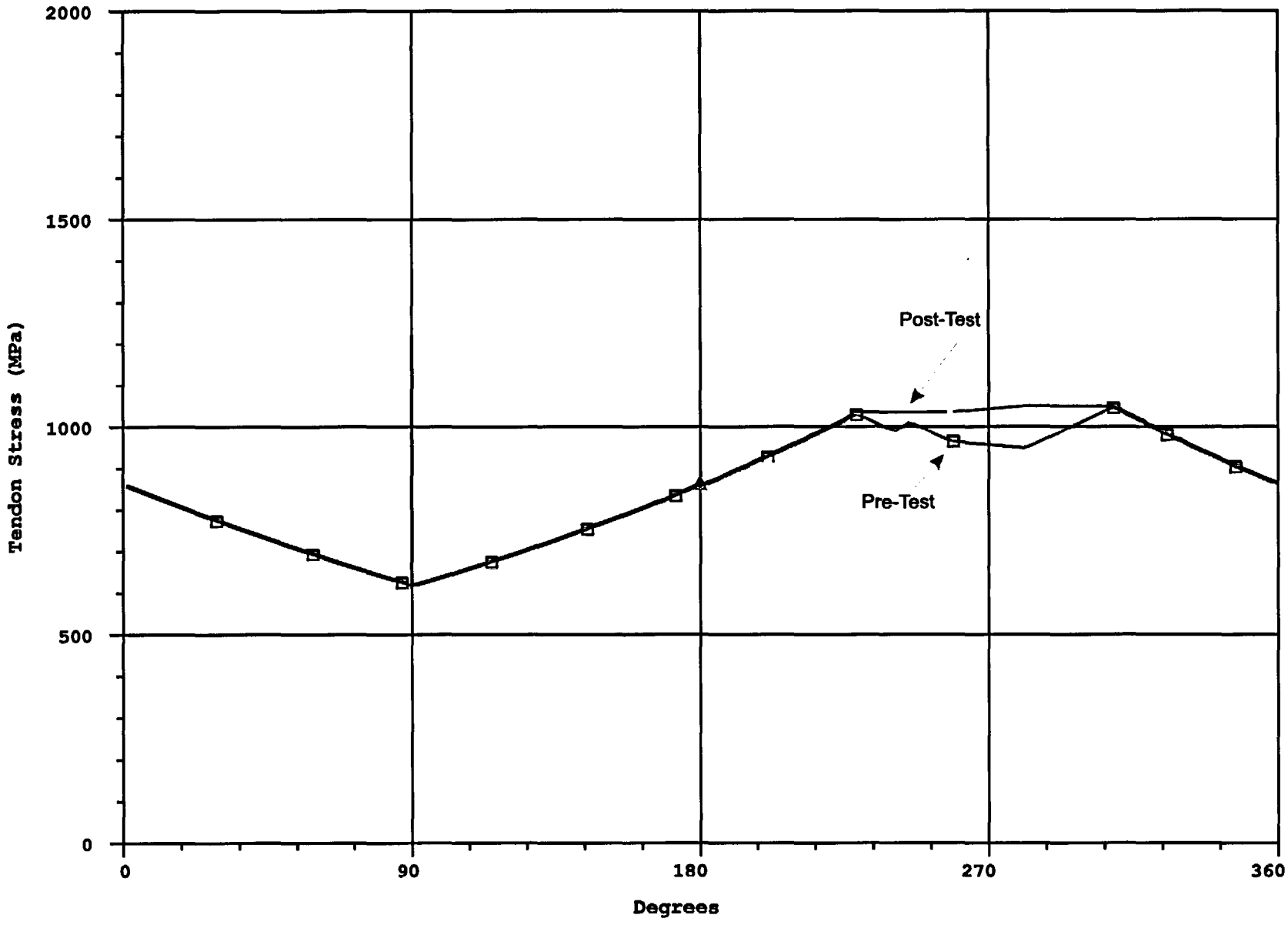

Figure 6-25. Changes to Anchor Set Prestress for Posttest 3DCM Study, Tendon H53

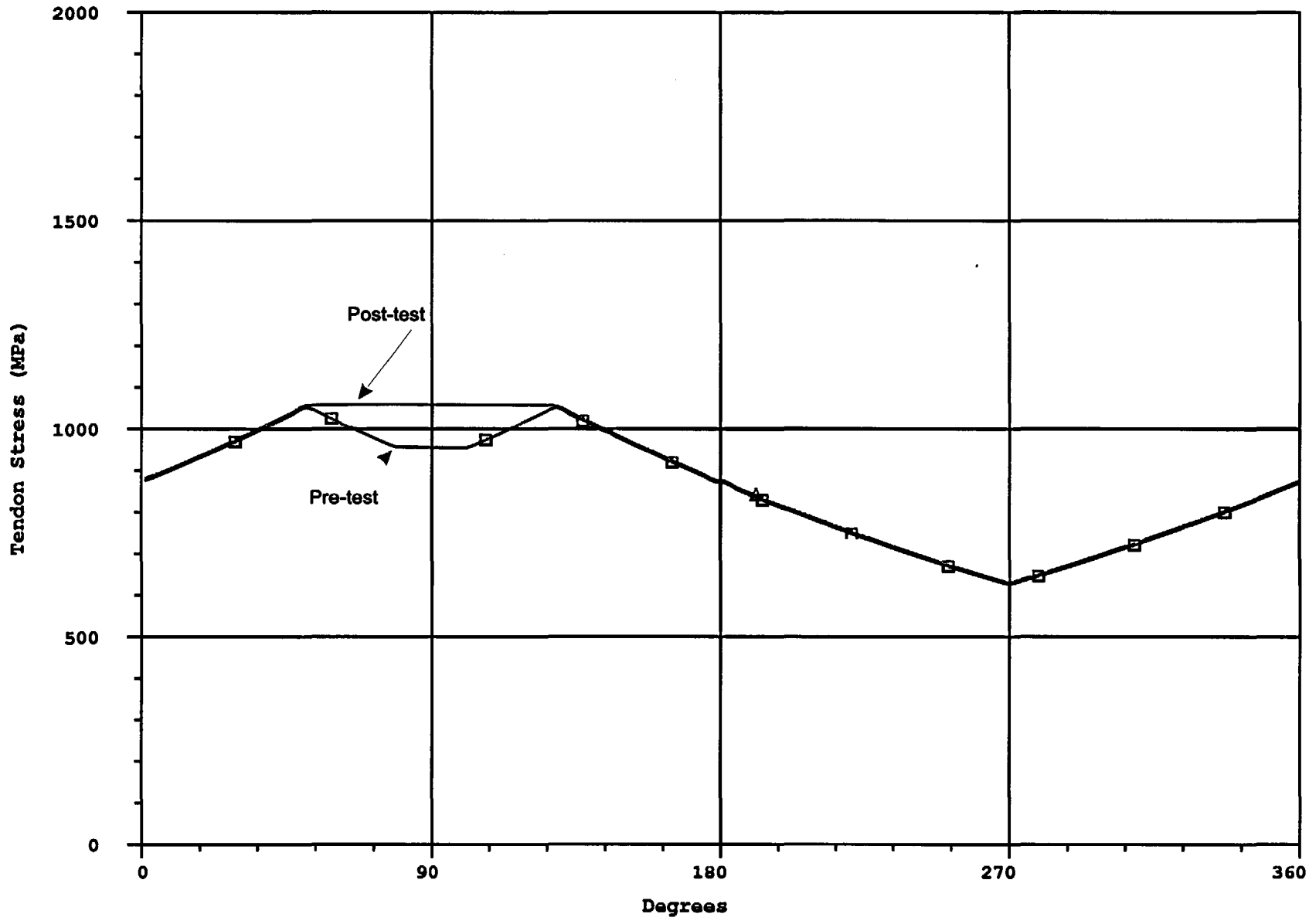

Figure 6-26. Changes to Anchor Set Prestress for Posttest 3DCM Study, Tendon H68

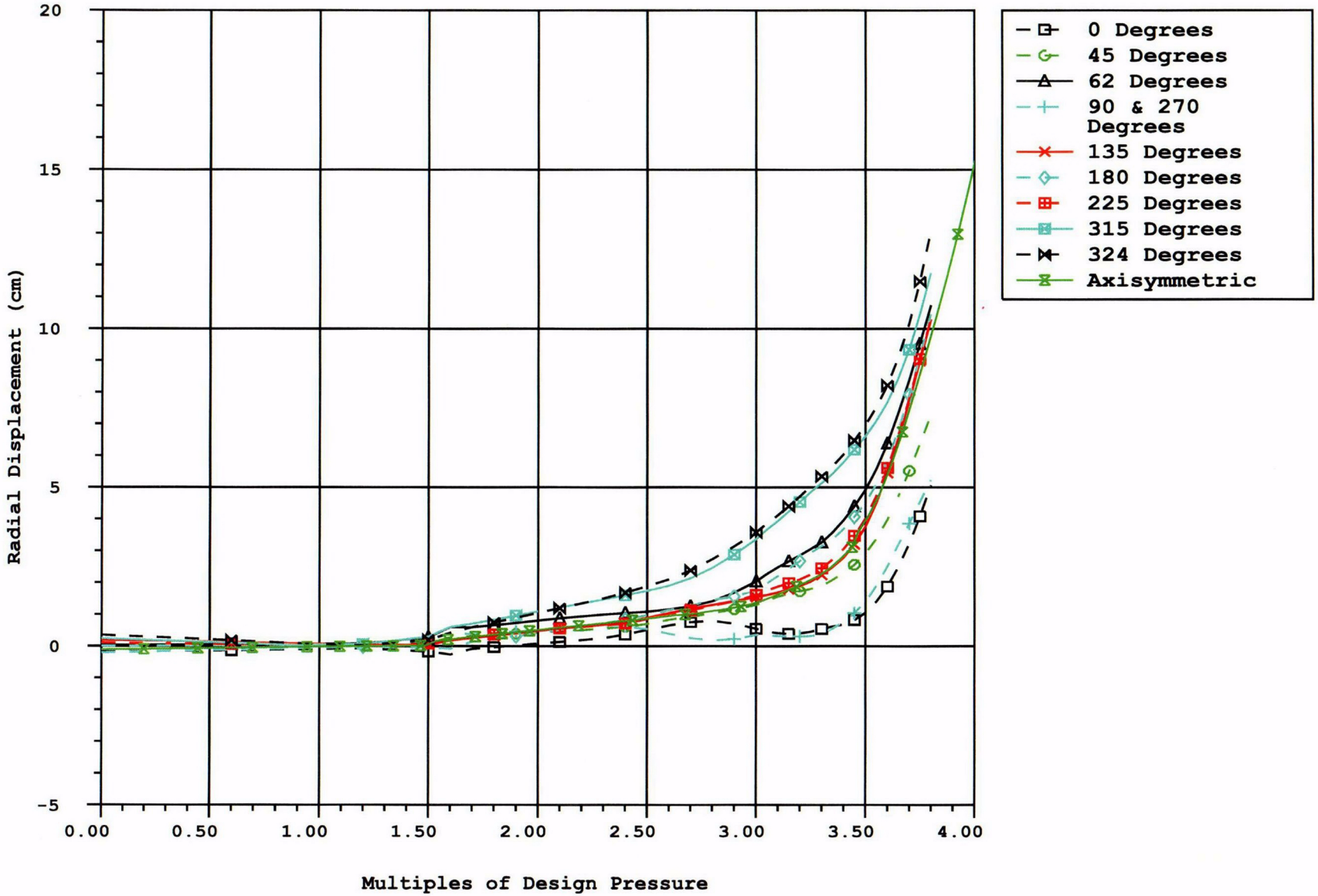

Figure 6-27. Radial Displacement at Elev. 4.7M, Posttest 3DCM Run 6 (Tendons "Bonded" After Prestressing) Compared to Axisymmetric

C121

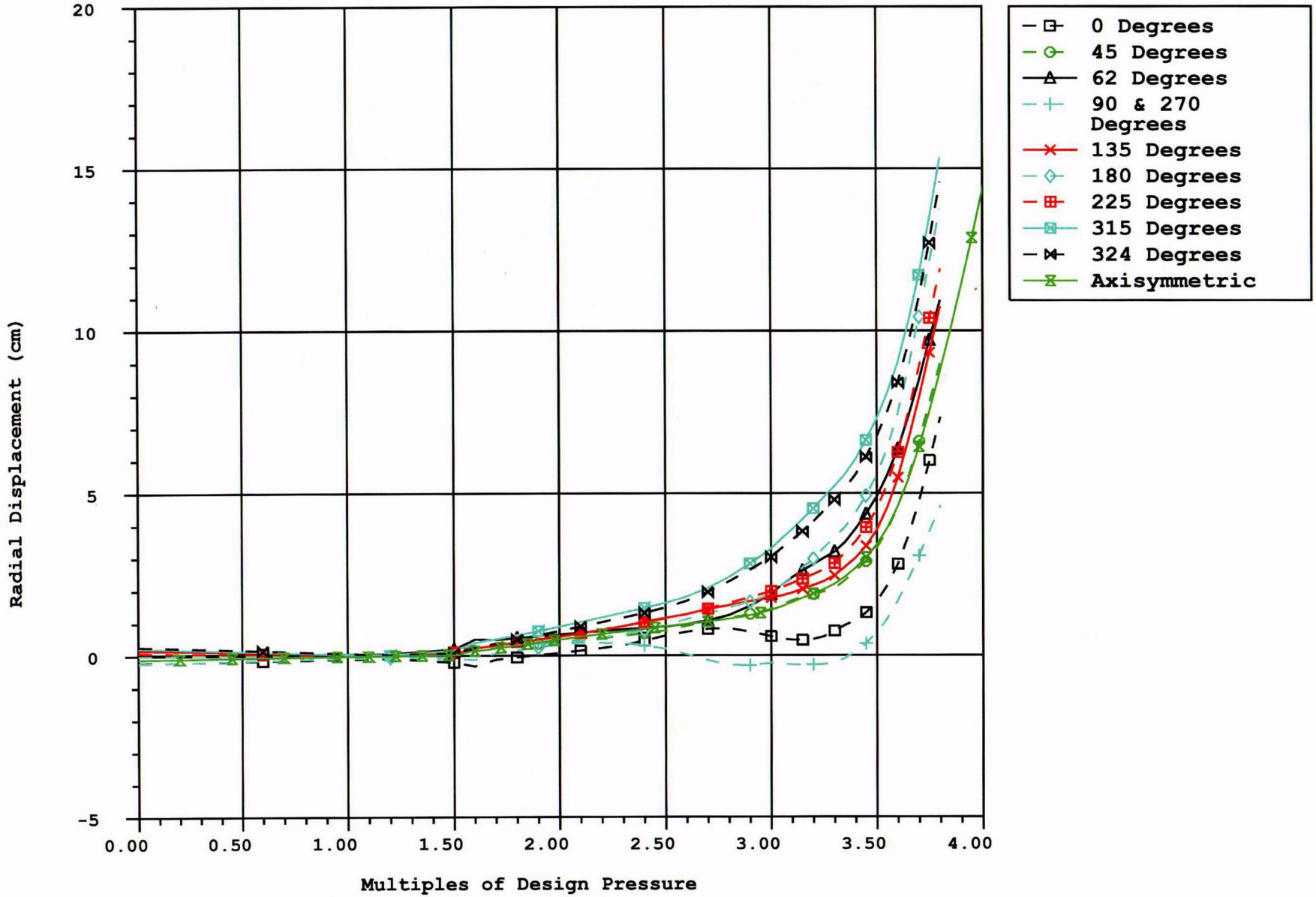

Figure 6-28. Radial Displacement at Elev. 6.2M, Posttest 3DCM Run 6 Compared to Axisymmetric

C122

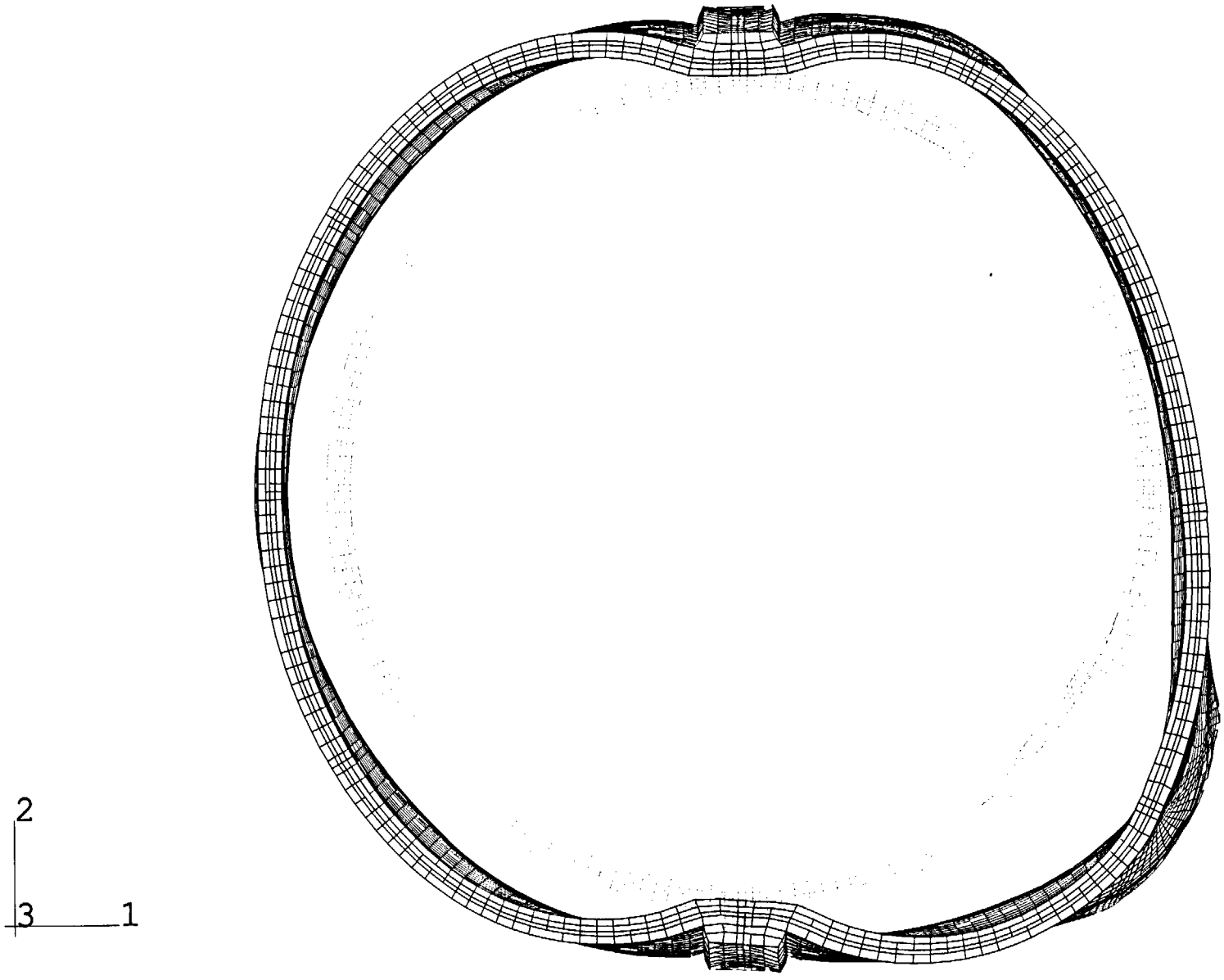

Figure 6-29. 3DCM Posttest Deformed Shape at P = 2.5Pd, Run 6 (mag. Factor = 100×)

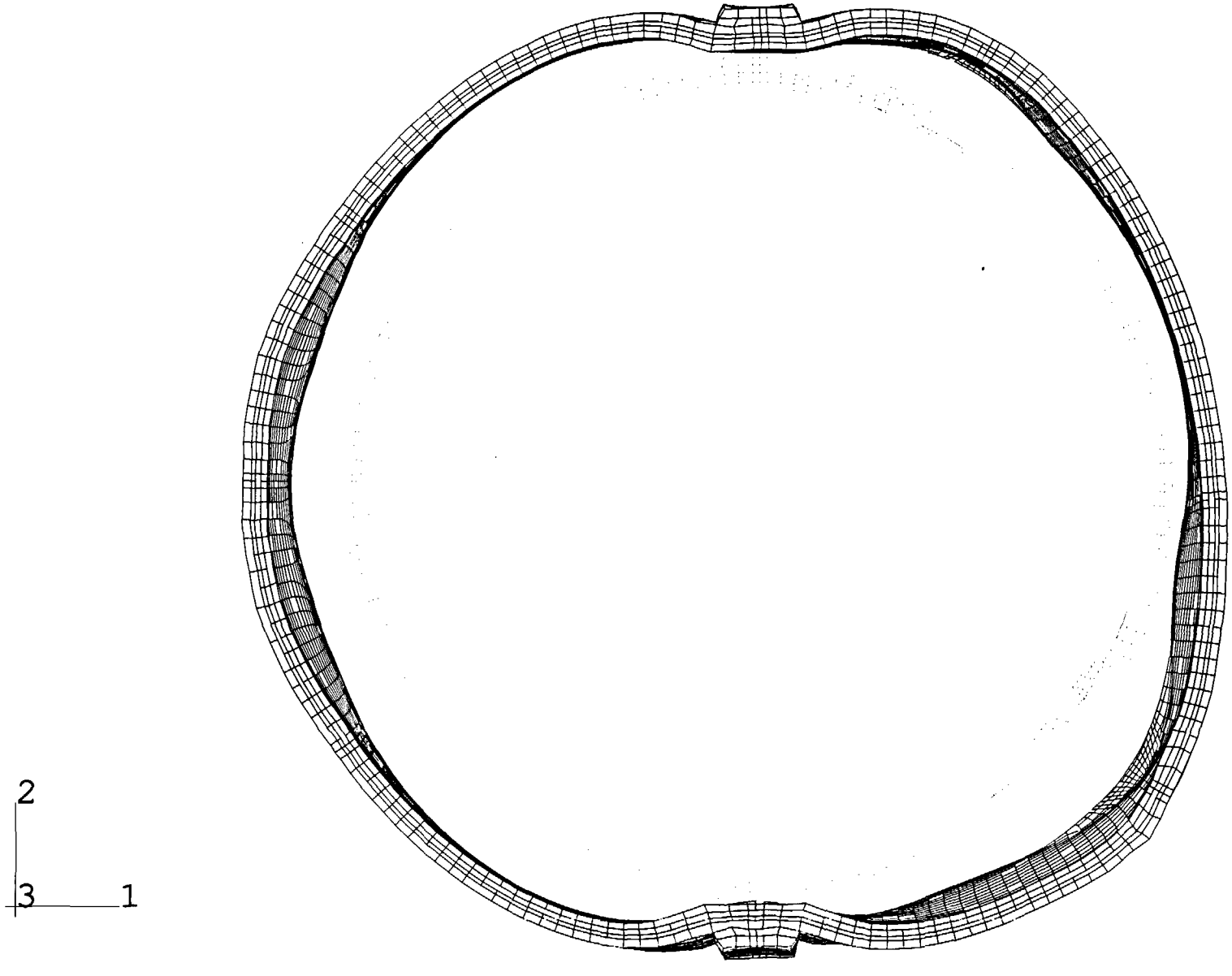

Figure 6-30. 3DCM Posttest Deformed Shape at P = 3.8Pd, Run 6 (mag. Factor = 10×)

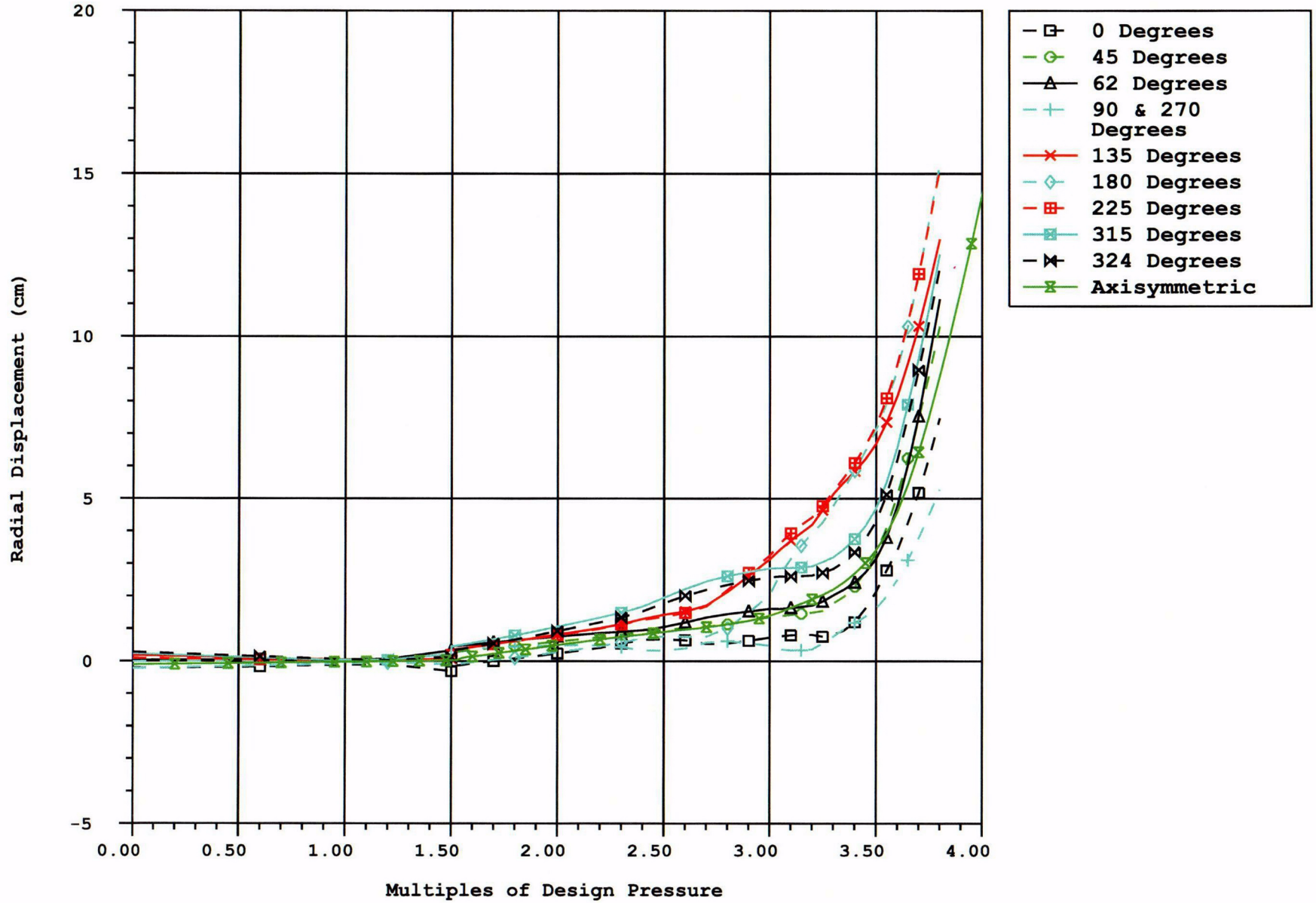

Figure 6-31. Radial Displacement at Elev. 6.2M, Posttest 3DCM Run 7 (No Friction After Prestress is Overcome) Compared to Axisymmetric

C123

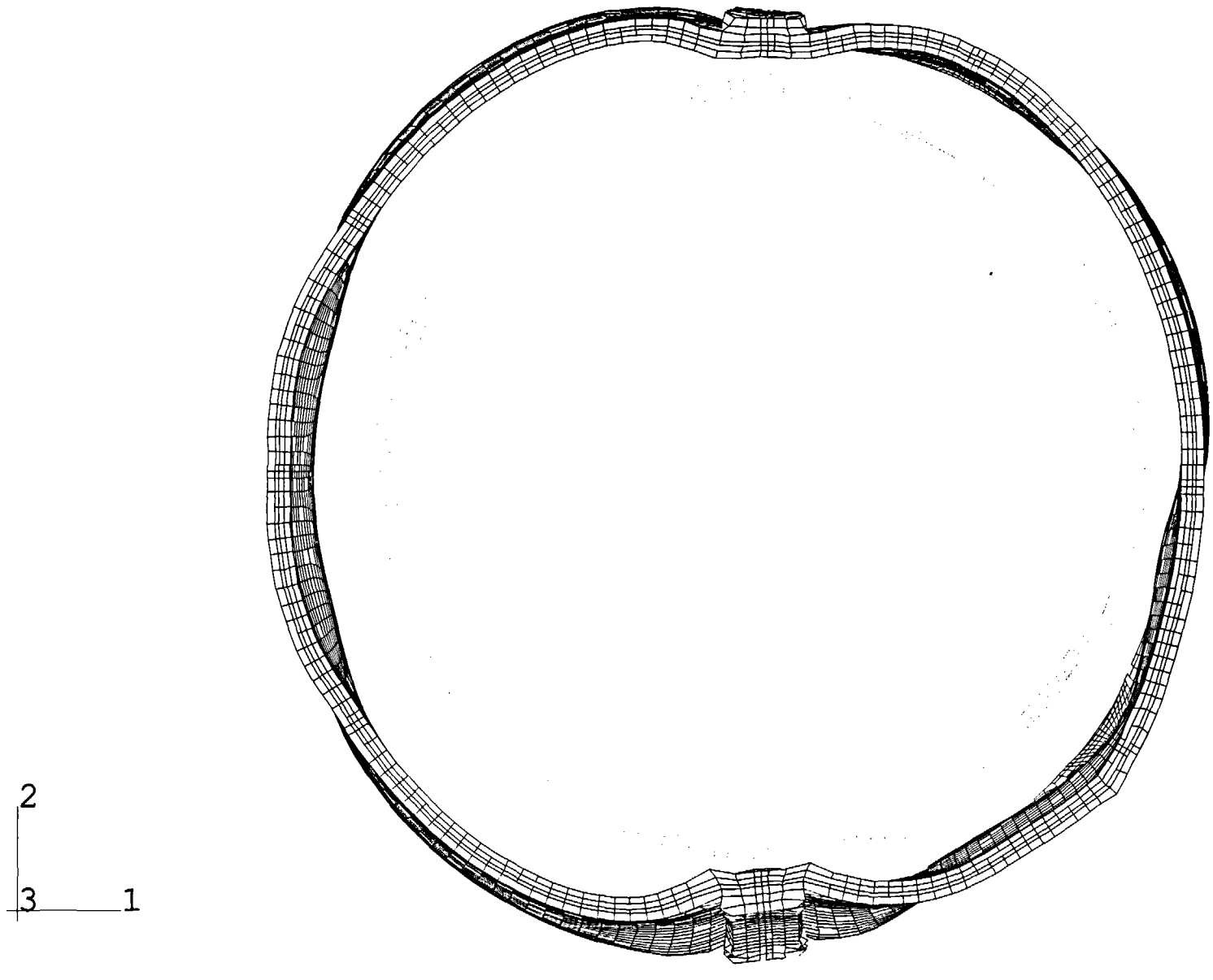

Figure 6-32. 3DCM Posttest Deformed Shape at P = 2.0 Pd, Run 7 (mag. Factor = 100×)

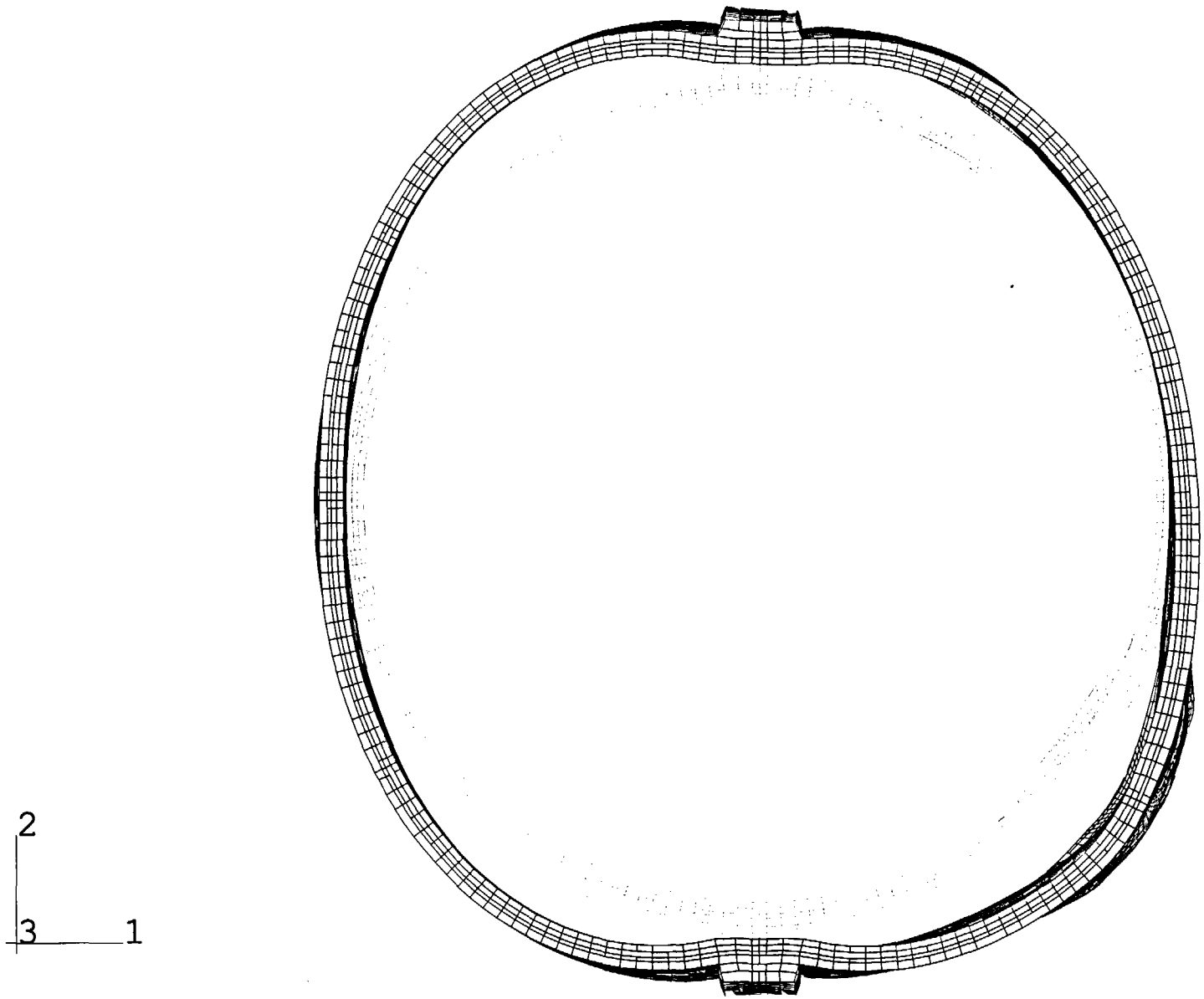

Figure 6-33. 3DCM Posttest Deformed Shape at P = 3.8 Pd, Run 7 (mag. Factor = 10×)

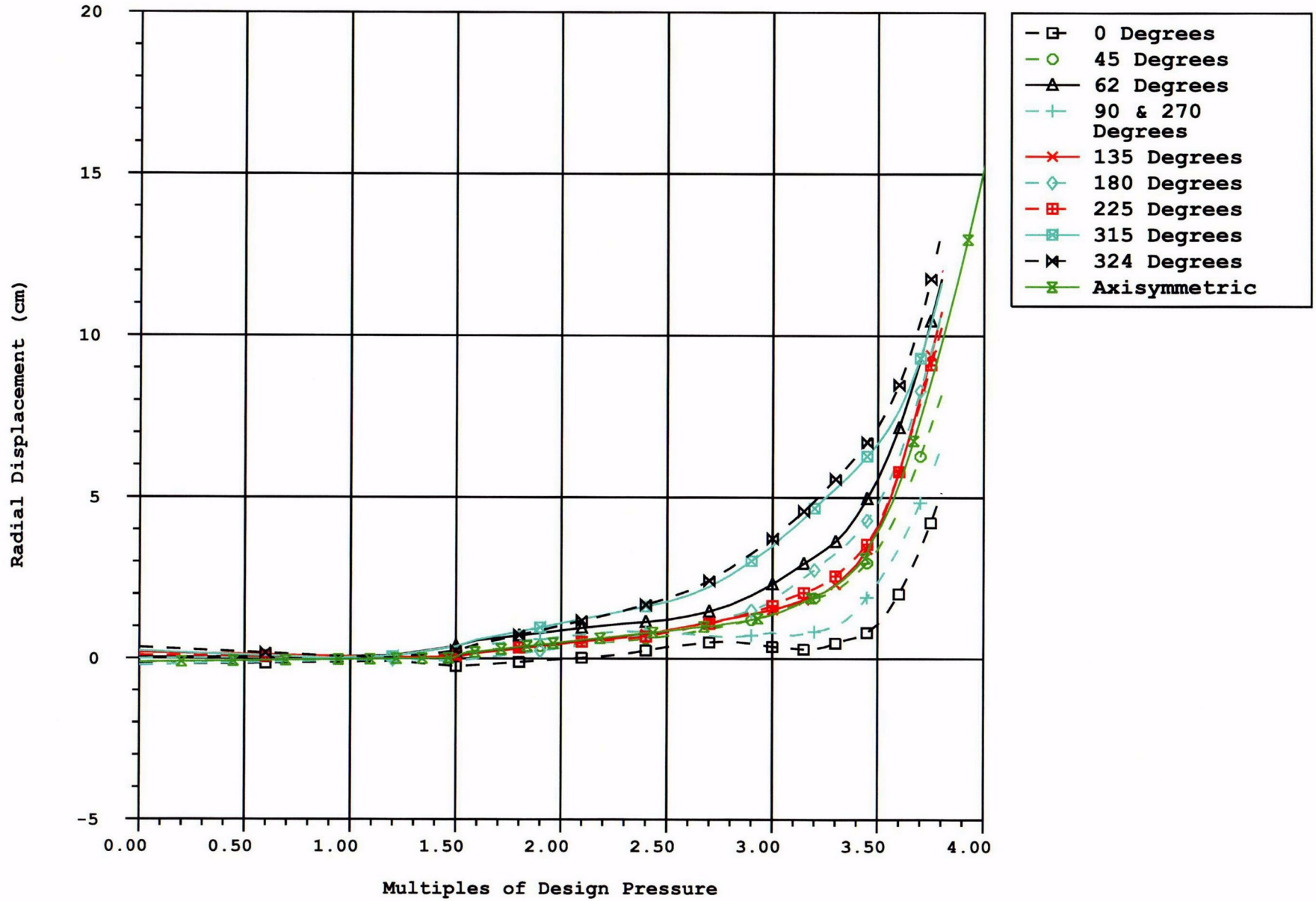

Figure 6-34. Radial Displacement at Elev. 4.7M, Posttest 3DCM Run 9 (Bi-directional Friction) Compared to Axisymmetric

C124

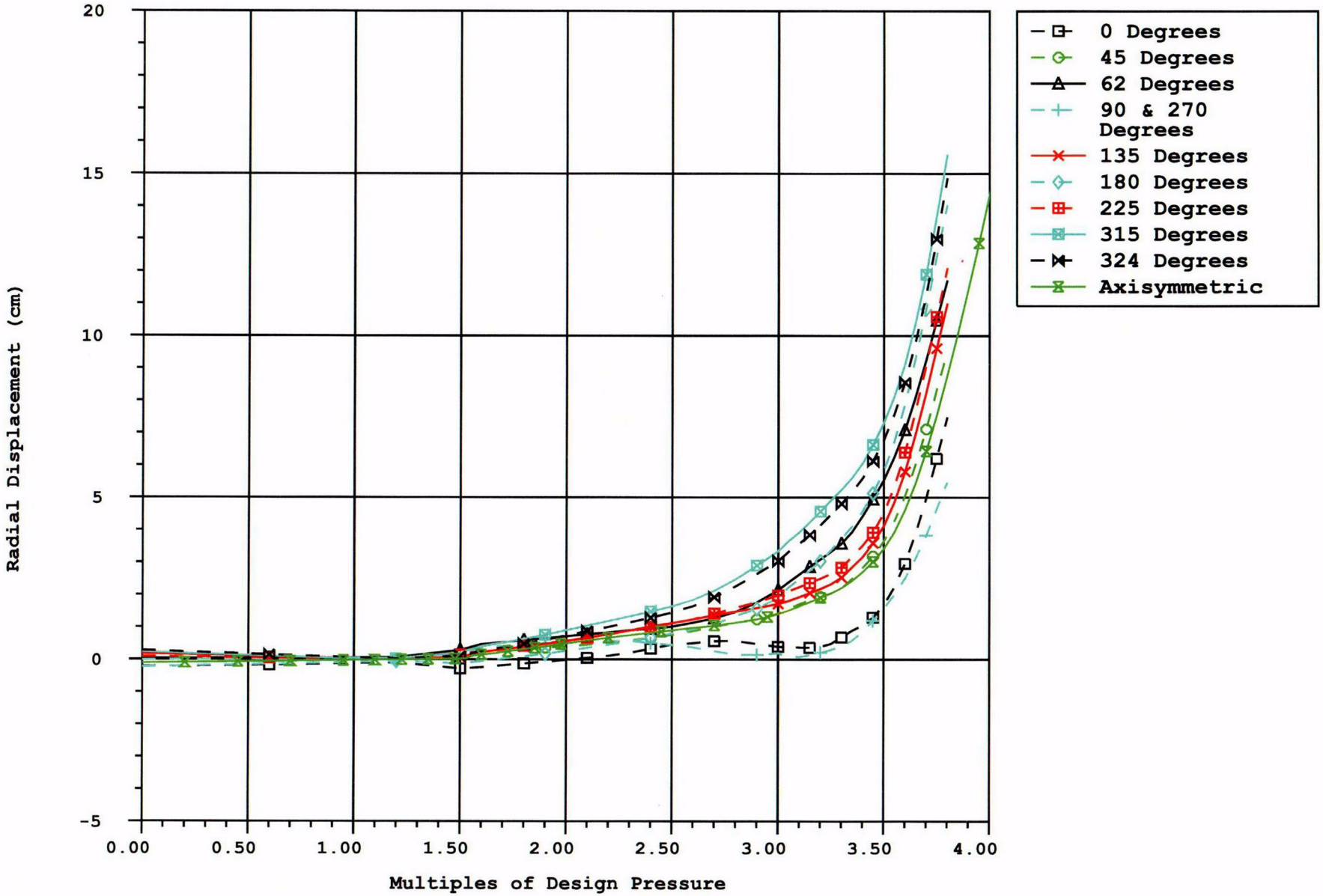

Figure 6-35. Radial Displacement at Elev. 6.2M, Posttest 3DCM Run 9 Compared to Axisymmetric

C125

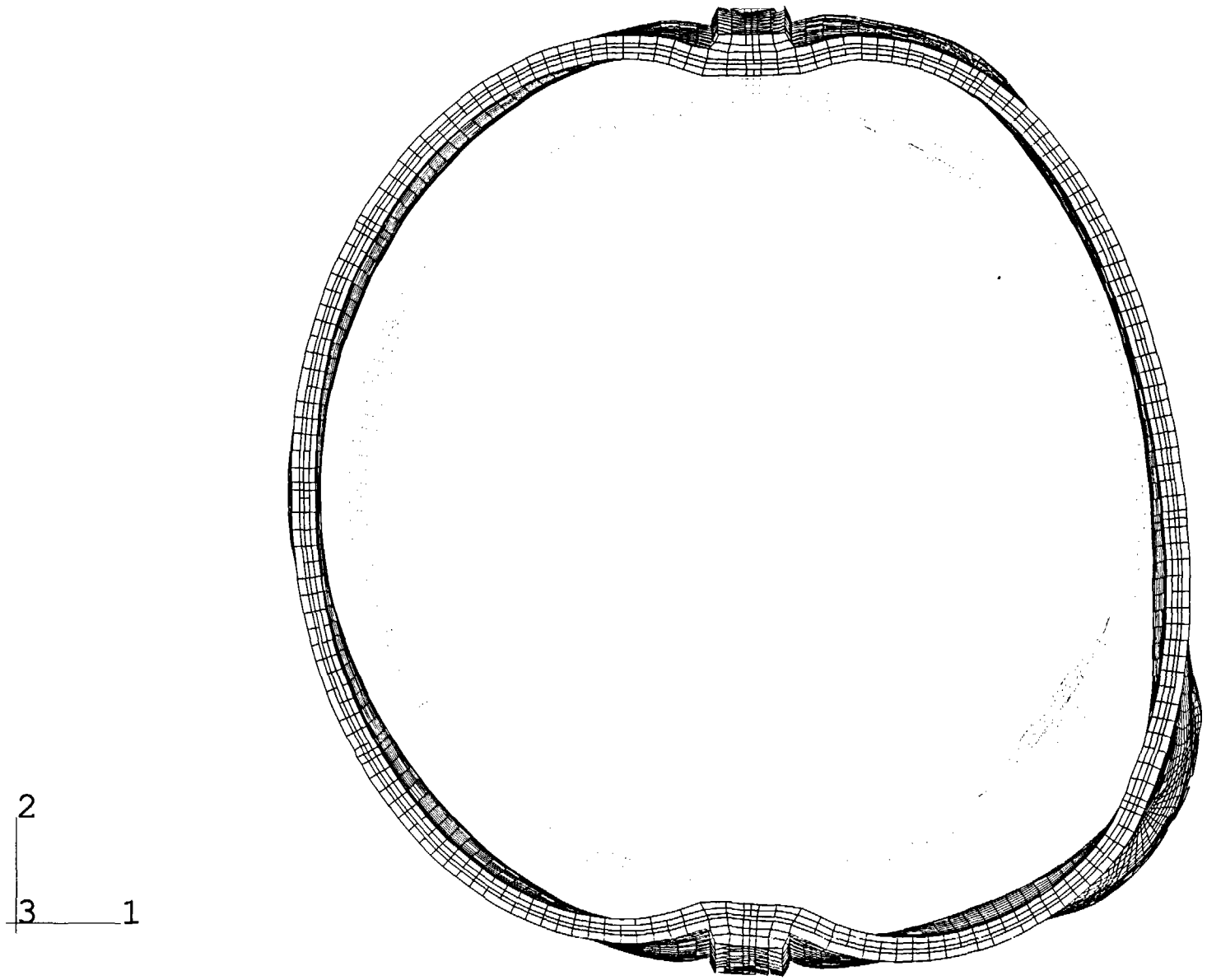

Figure 6-36. 3DCM Posttest Deformed Shape at P = 2.5 Pd, Run 9 (mag. Factor = 100×)

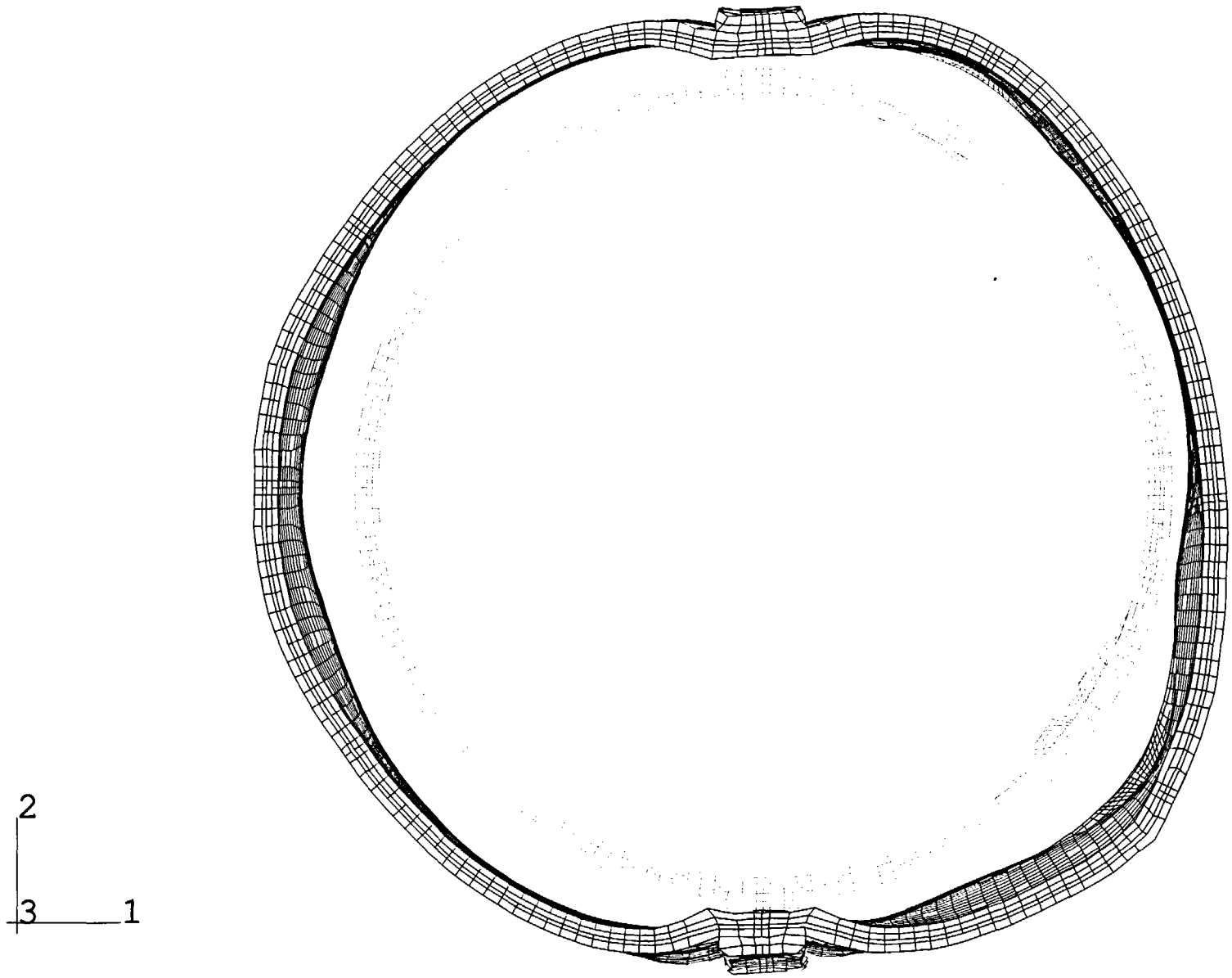

Figure 6-37. 3DCM Posttest Deformed Shape at P = 3.8 Pd, Run 9 (mag. Factor = 10×)

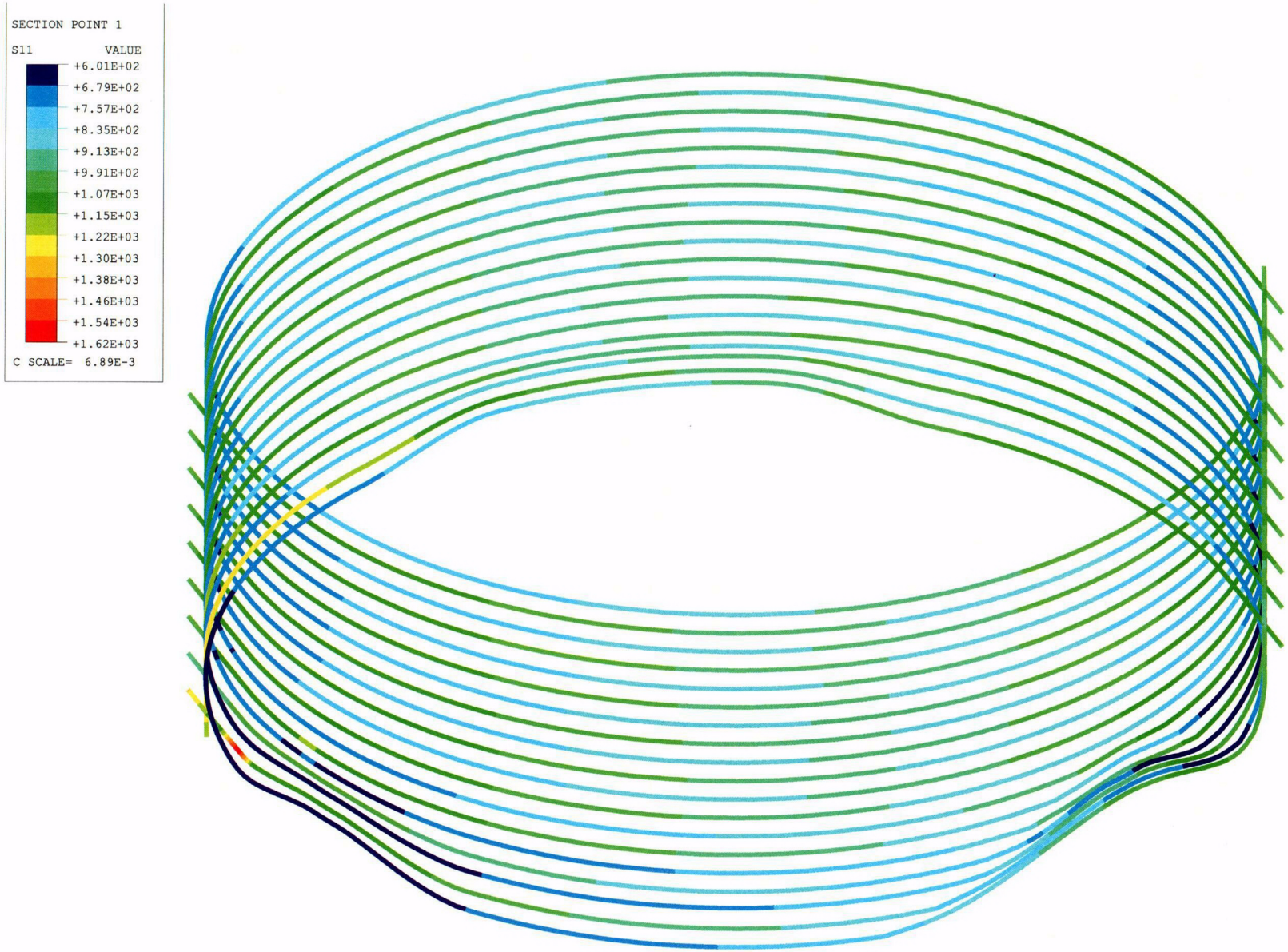

Figure 6-38. 3DCM Posttest Tendon Stress Contours at P = 1.5 Pd, Run 6

C126

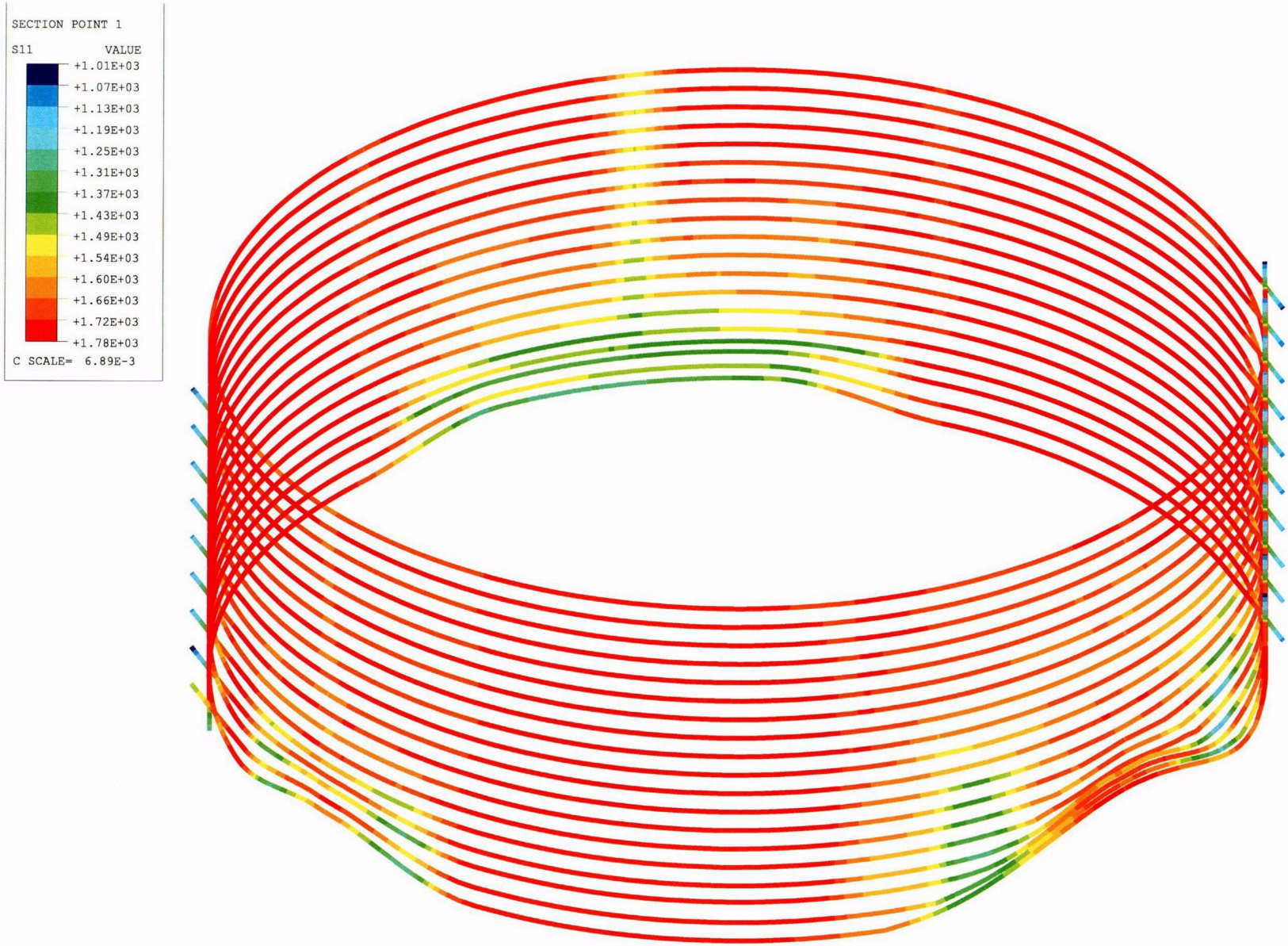

Figure 6-39. 3DCM Posttest Tendon Stress Contours at P = 3.5 Pd, Run 6

C127

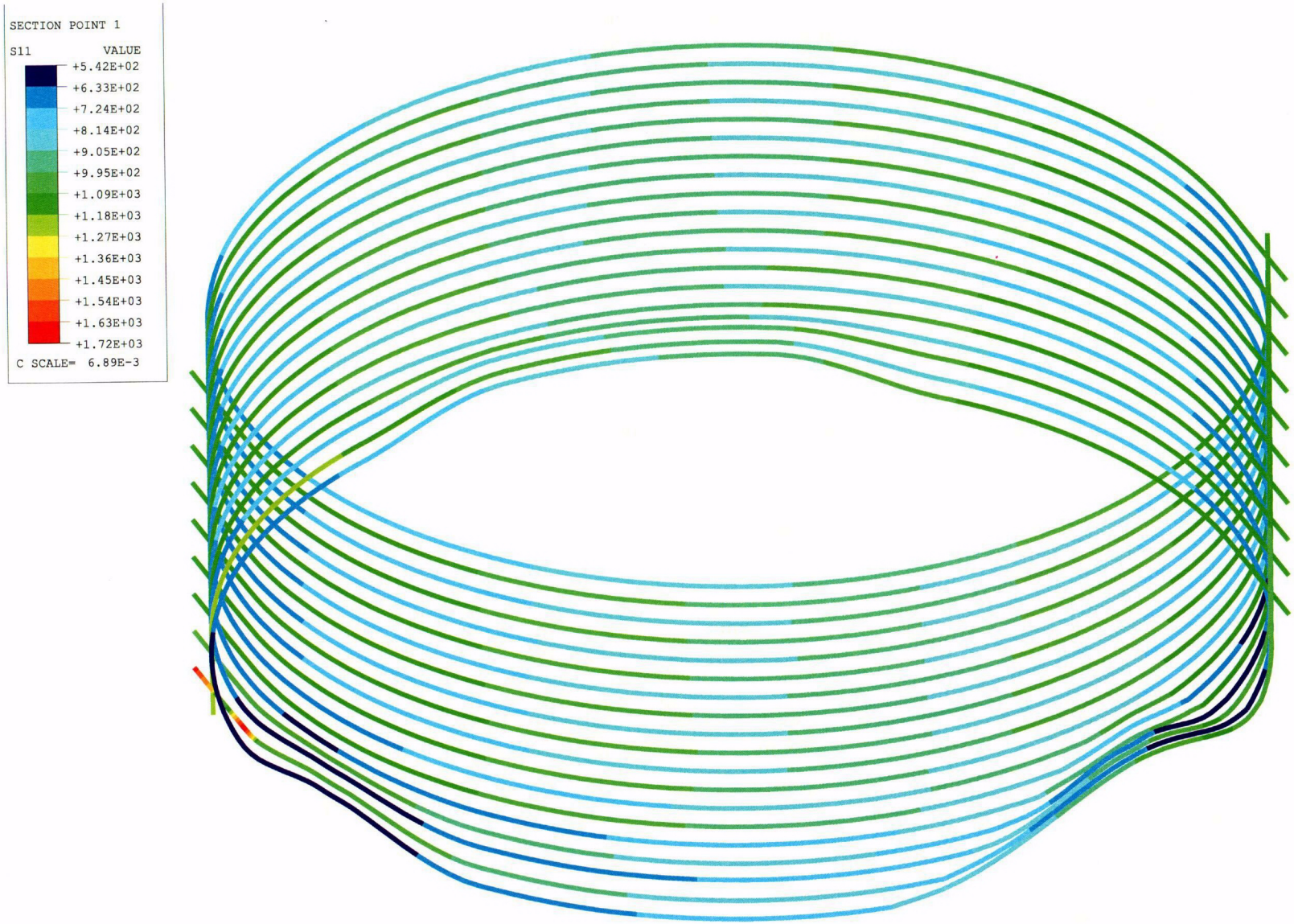

Figure 6-40. 3DCM Posttest Tendon Stress Contours at P = 1.5 Pd, Run 7, Before Friction Element Modeling Modification

C128

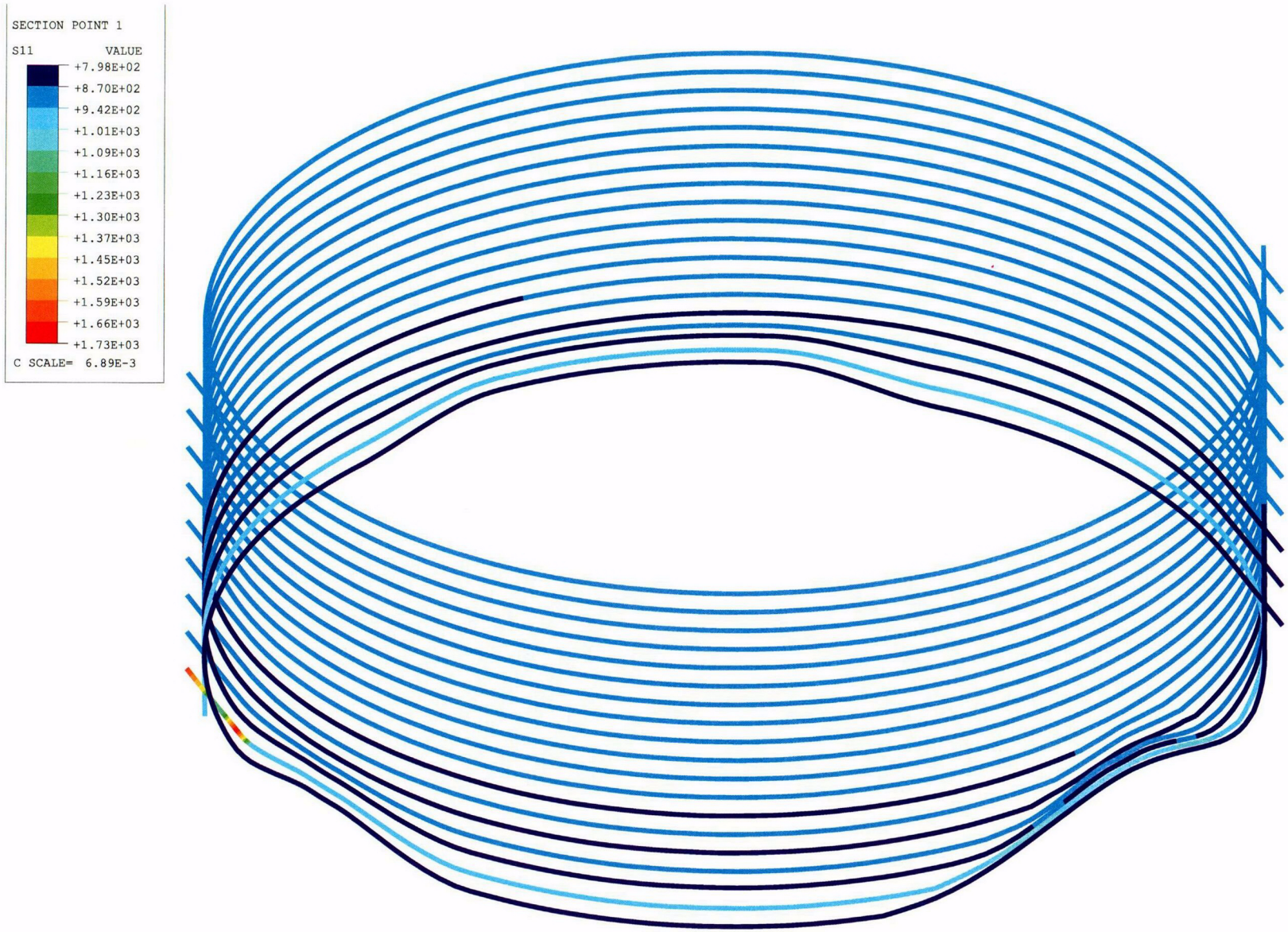

Figure 6-41. 3DCM Posttest Tendon Stress Contours at P = 1.5 Pd, Run 7, After Friction Element Modeling Modification

C129

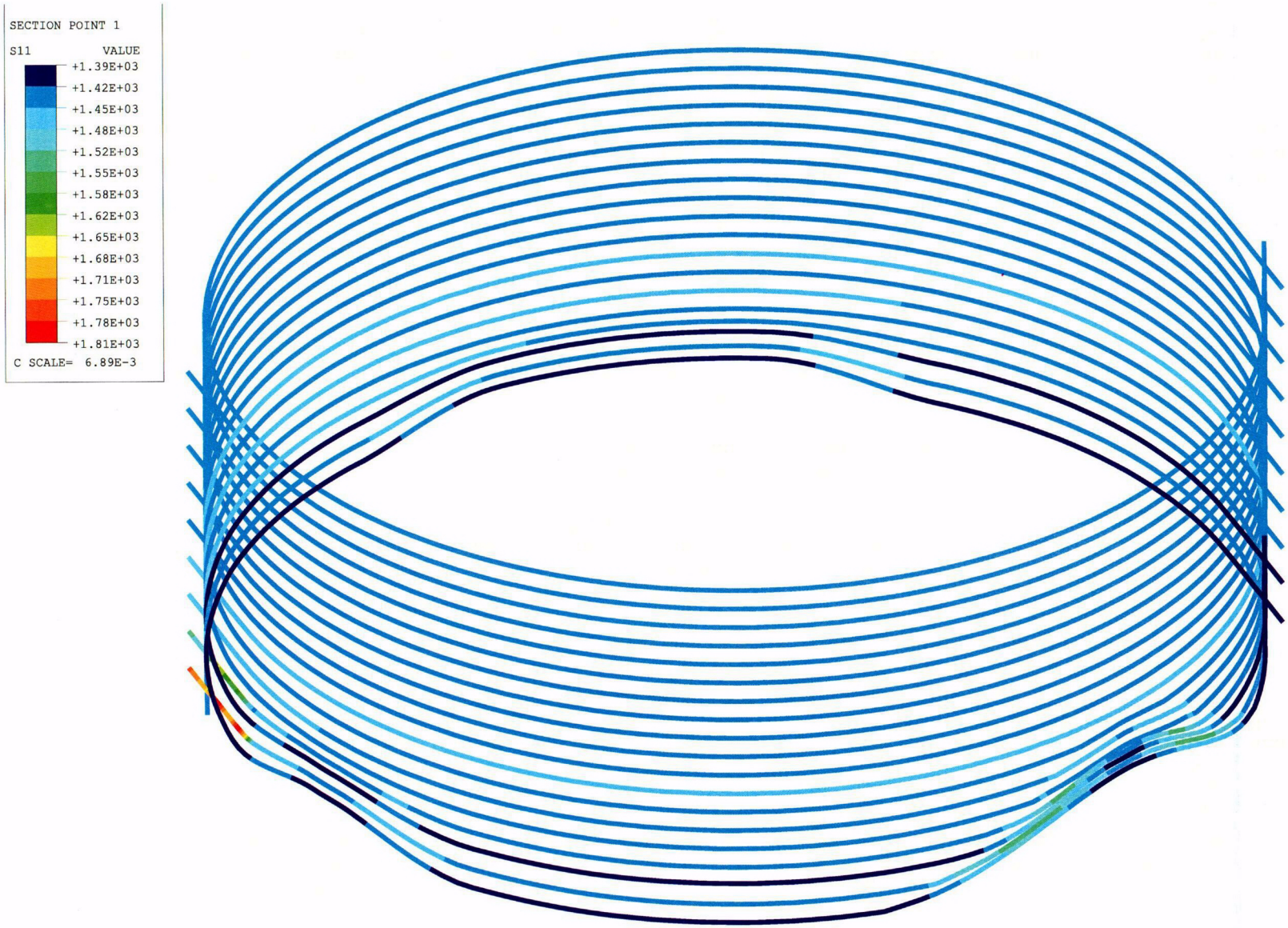

Figure 6-42. 3DCM Posttest Tendon Stress Contours at P = 3.5 Pd, Run 7

C130